University of Zurich[UZH]
Physik-Institut

High-p_T multi-jet final states at ATLAS and CMS

searching for new phenomena beyond 1 TeV at $\sqrt{s}$ = 13 TeV

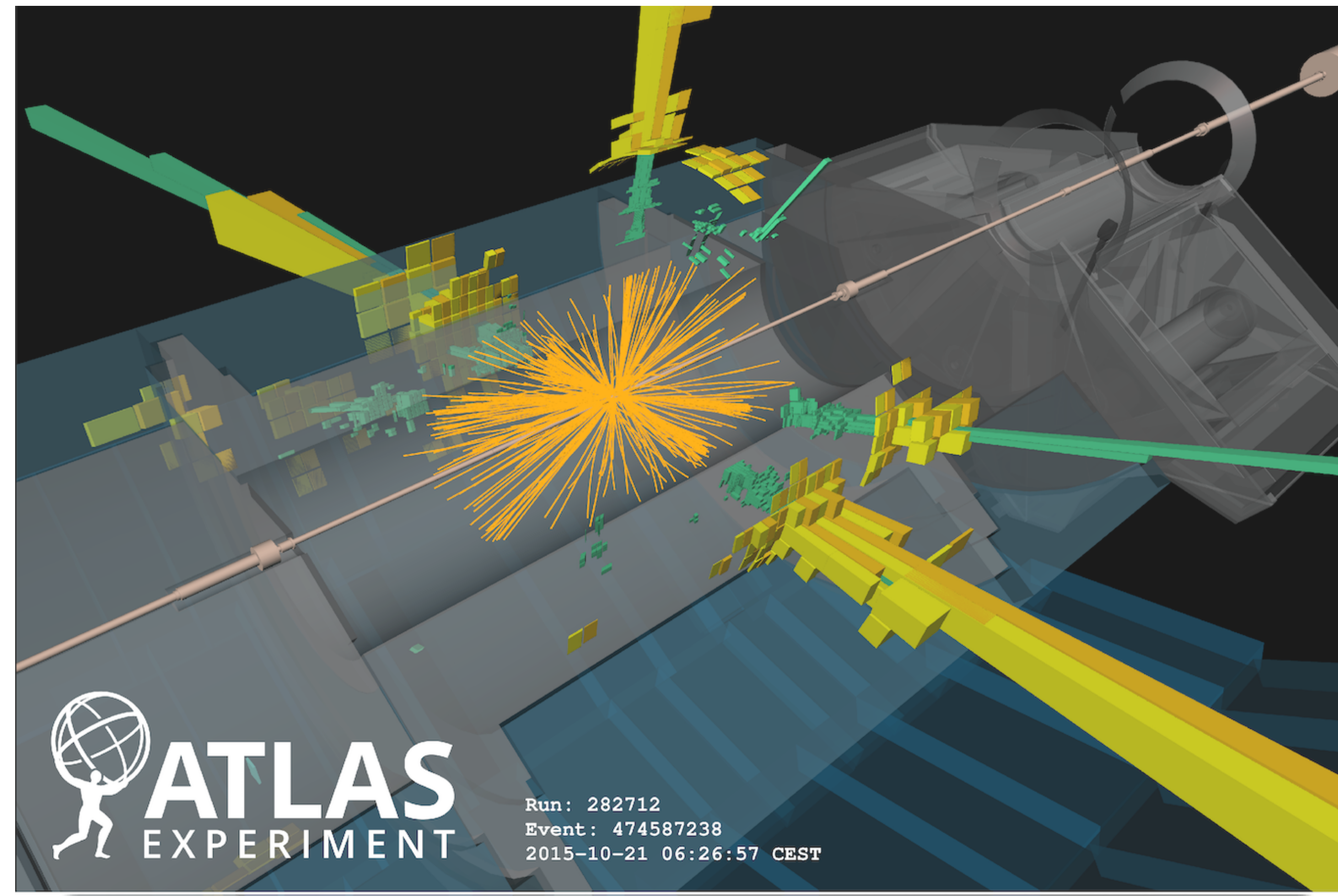

Clemens Lange (UZH)
on behalf of the ATLAS and CMS collaborations

51st Rencontres de Moriond on
"Electroweak Interactions and Unified Theories"
La Thuile, Italy
12th-19th March 2016

advancing to √s = 13 TeV

- increased centre-of-mass energy of the LHC opened up a **new energy regime**
- final states including partons often dominate beyond standard model (BSM) phenomena
- these are observed as **multi-jet final states** in the detector

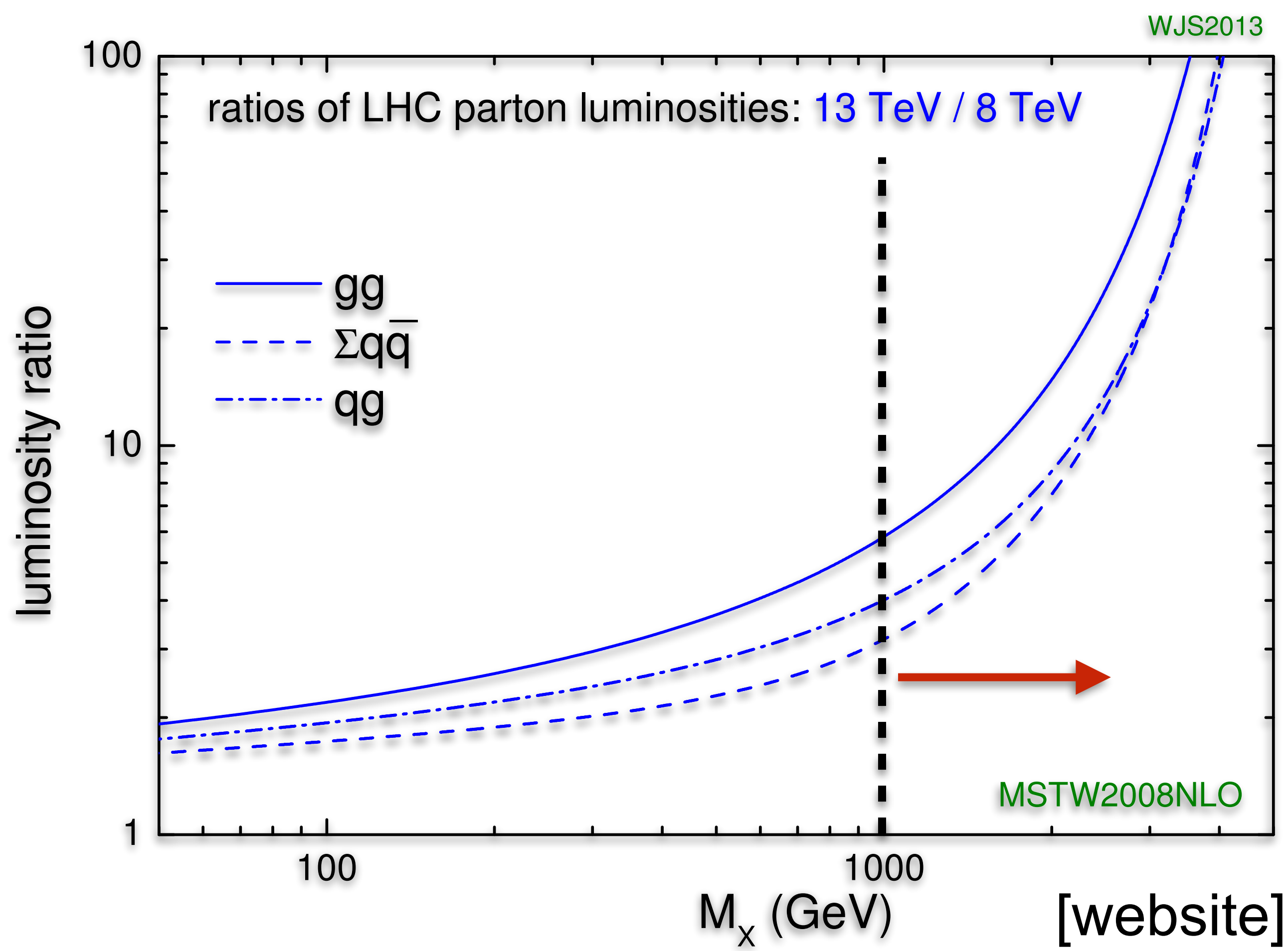

[website]

how do multi-jet resonances relate to the di-photon excitement?

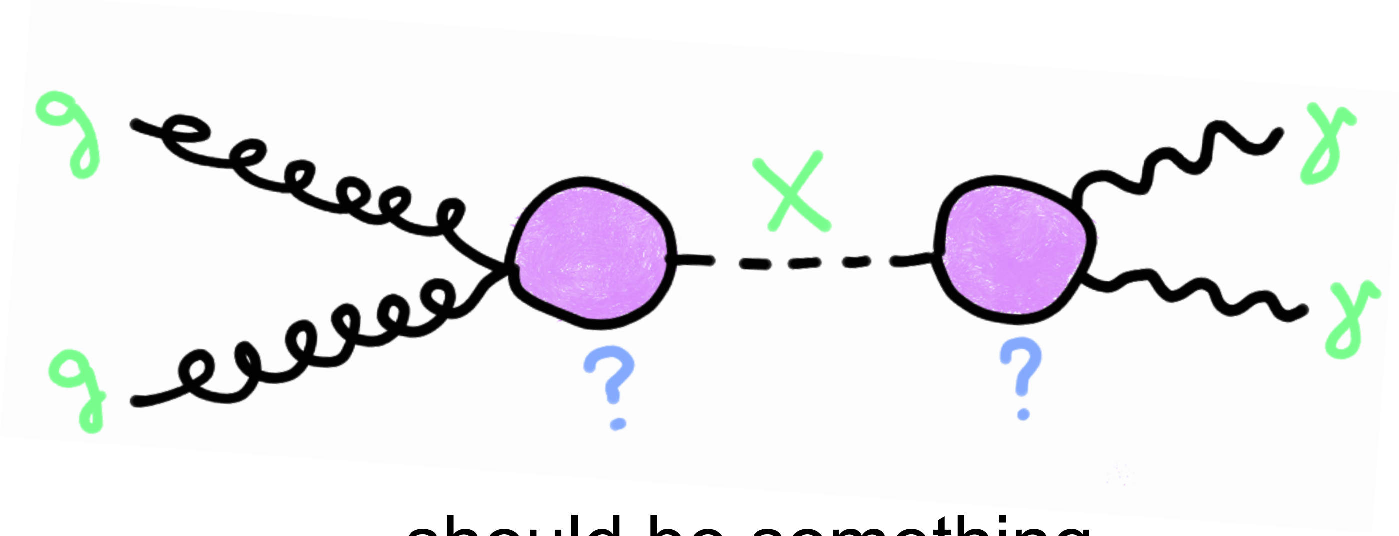

?

should be something
coloured and **charged**
in production and decay

- neutral resonance cannot directly couple to photons ➜ loop of **charged particles** (e.g. W, top, ?) **in decay** (and production?)
- there must be **more than just a di-photon resonance**
- searches presented in this talk **constrain** what **physics models** this potential resonance could be

multi-jet final states with and without leptons

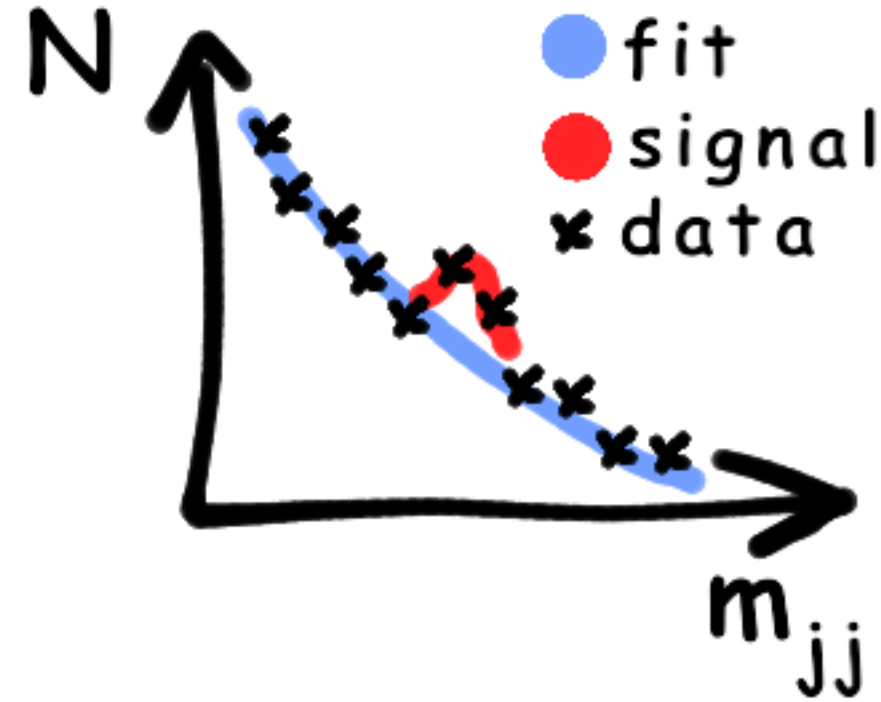

- major **difference** between **pure multi-jet** final states and **final states with leptons**: background estimation methods
- 0-lepton final states:
  - dominated by QCD multi-jet events
  - mostly **use functional forms** for background estimation
- leptons+jets final states:
  - multi-jet background significantly reduced by requiring presence of lepton
  - different composition of background processes, not necessarily one dominant
  - **estimate individual background components**

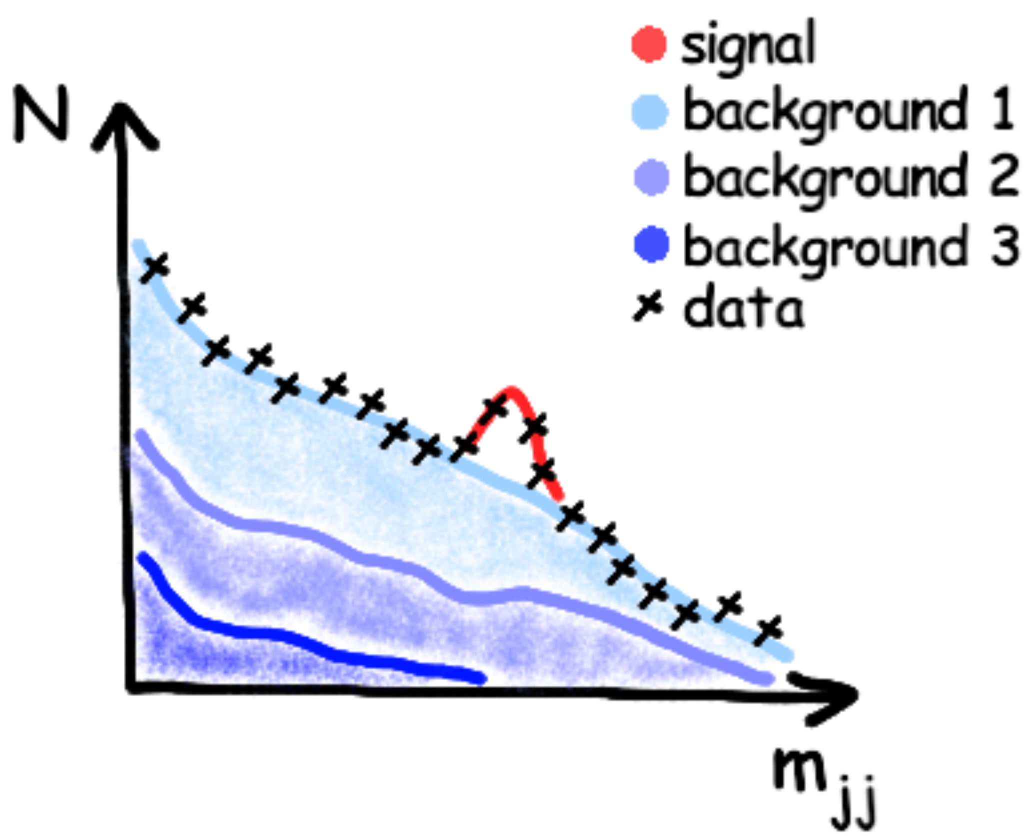

0-lepton (and multi-jet background dominated) final states

Search for (narrow) di-jet resonances & new phenomena in di-jet angular distributions (ATLAS & CMS)

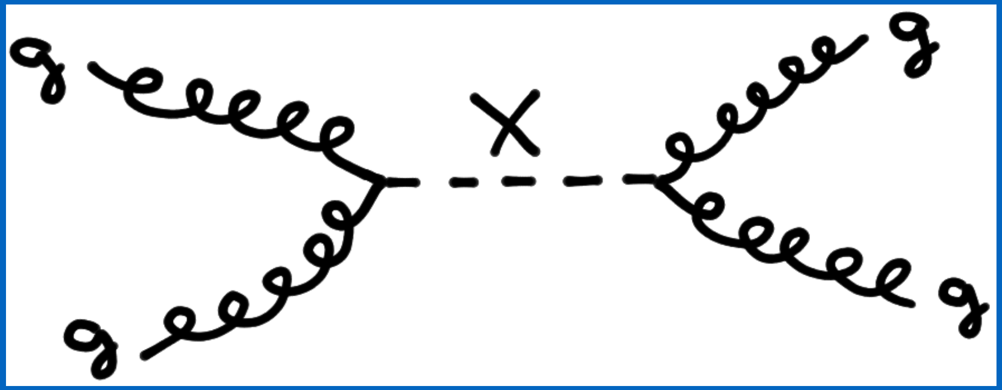

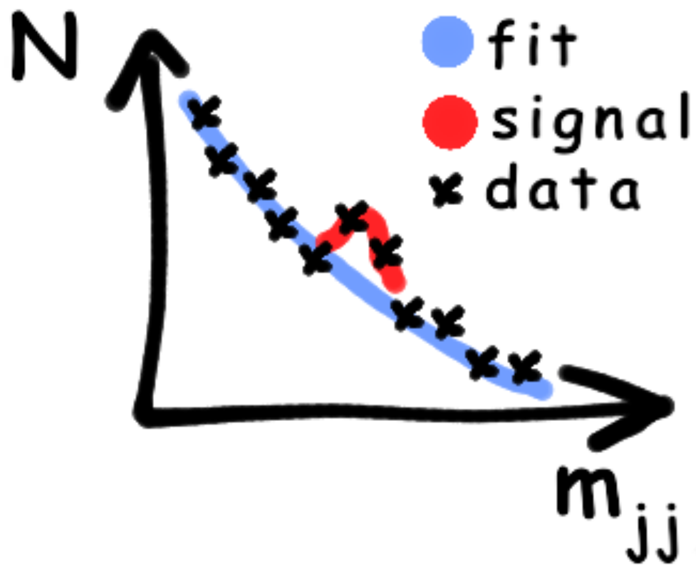

Search for resonances in di-jet events with one or two identified b-jets (ATLAS)

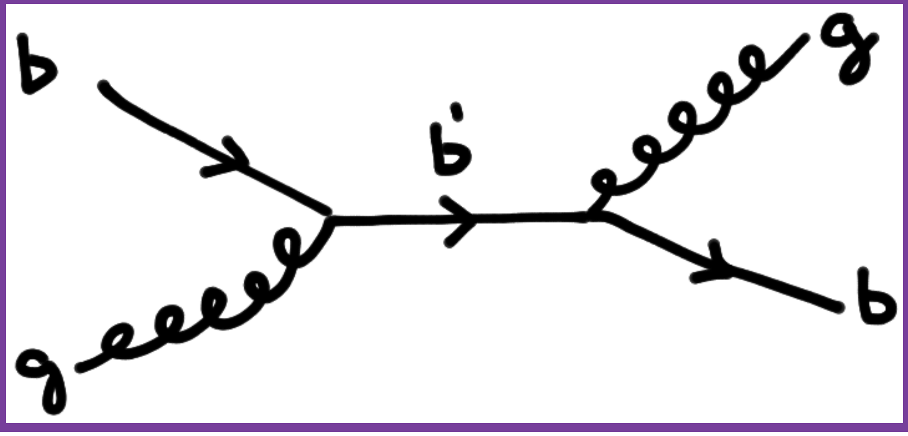

Search for strong gravity/black holes in multi-jet final states (ATLAS & CMS)

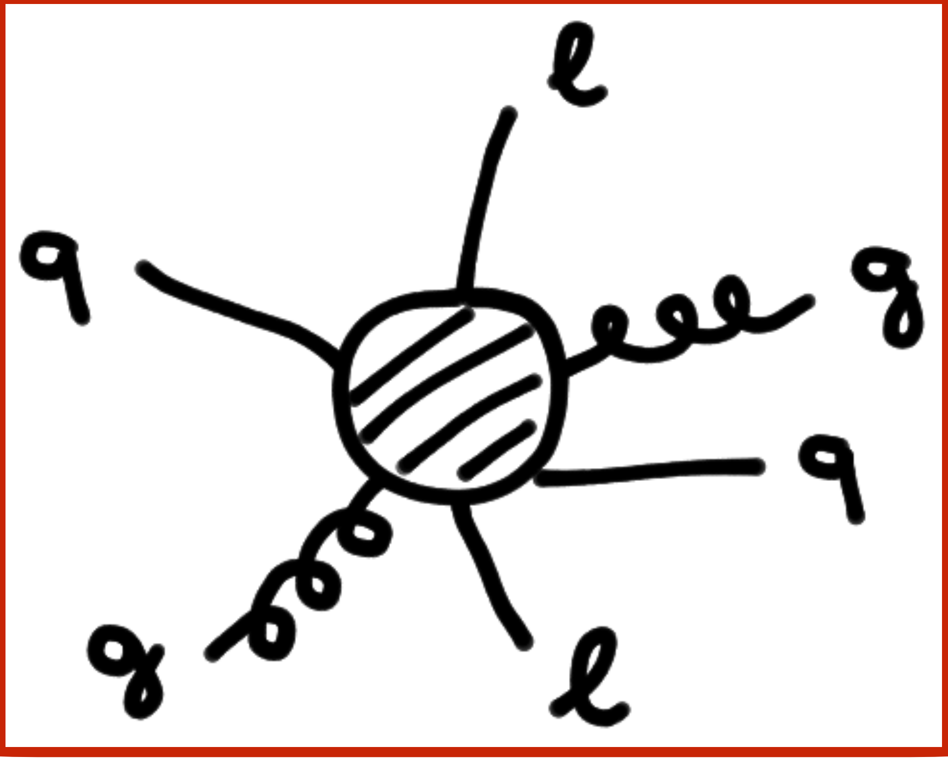

how to perform a bump hunt

- background functional form mostly chosen arbitrarily
- assume **falling spectrum**
- **define procedure** to choose **functional form** and **number of parameters** based on statistical tests
- need to account for potential bias
- MC simulated events used for validation

	Functional form	p_1	p_2
1	$f_1(x) = \frac{p_0(1-x)^{p_1}}{x^{p_2}}$	$(0,+\infty)$	$(0,+\infty)$
2	$f_2(x) = p_0(1-x)^{p_1} e^{p_2 x^2}$	$(0,+\infty)$	$(-\infty,+\infty)$
3	$f_3(x) = p_0(1-x)^{p_1} x^{p_2 x}$	$(0,+\infty)$	$(-\infty,+\infty)$
4	$f_4(x) = p_0(1-x)^{p_1} x^{p_2 \ln x}$	$(0,+\infty)$	$(-\infty,+\infty)$
5	$f_5(x) = p_0(1-x)^{p_1} (1+x)^{p_2 x}$	$(0,+\infty)$	$(0,+\infty)$
6	$f_6(x) = p_0(1-x)^{p_1} (1+x)^{p_2 \ln x}$	$(0,+\infty)$	$(0,+\infty)$
7	$f_7(x) = \frac{p_0}{x}(1-x)^{[p_1 - p_2 \ln x]}$	$(0,+\infty)$	$(0,+\infty)$
8	$f_8(x) = \frac{p_0}{x^2}(1-x)^{[p_1 - p_2 \ln x]}$	$(0,+\infty)$	$(0,+\infty)$
9	$f_9(x) = \frac{p_0(1-x^{1/3})^{p_1}}{x^{p_2}}$	$(0,+\infty)$	$(0,+\infty)$
10	$f_{10}(x) = p_0(1-x^{1/3})^{p_1} x^{p_2 \ln x}$	$(0,+\infty)$	$(-\infty,+\infty)$

arXiv:1512.02586

CMS di-jet function:

$$\frac{d\sigma}{dm_{jj}} = \frac{P_0(1-x)^{P_1}}{x^{P_2+P_3 \ln(x)}}$$

di-jet resonance and angular analysis selection

cut	ATLAS	CMS
trigger	jet p_T > 360 GeV	jet p_T > 500 GeV or H_T > 800 GeV
offline	jet1 p_T > 440 GeV jet2 p_T > 50 GeV $\|y^*\| < 1.7$ (99.5% trigger eff.)	p_T > 30 GeV m_{jj} > 1.2 TeV $\|\Delta\eta_{jj}\| < 1.3$ (100% trigger eff.)

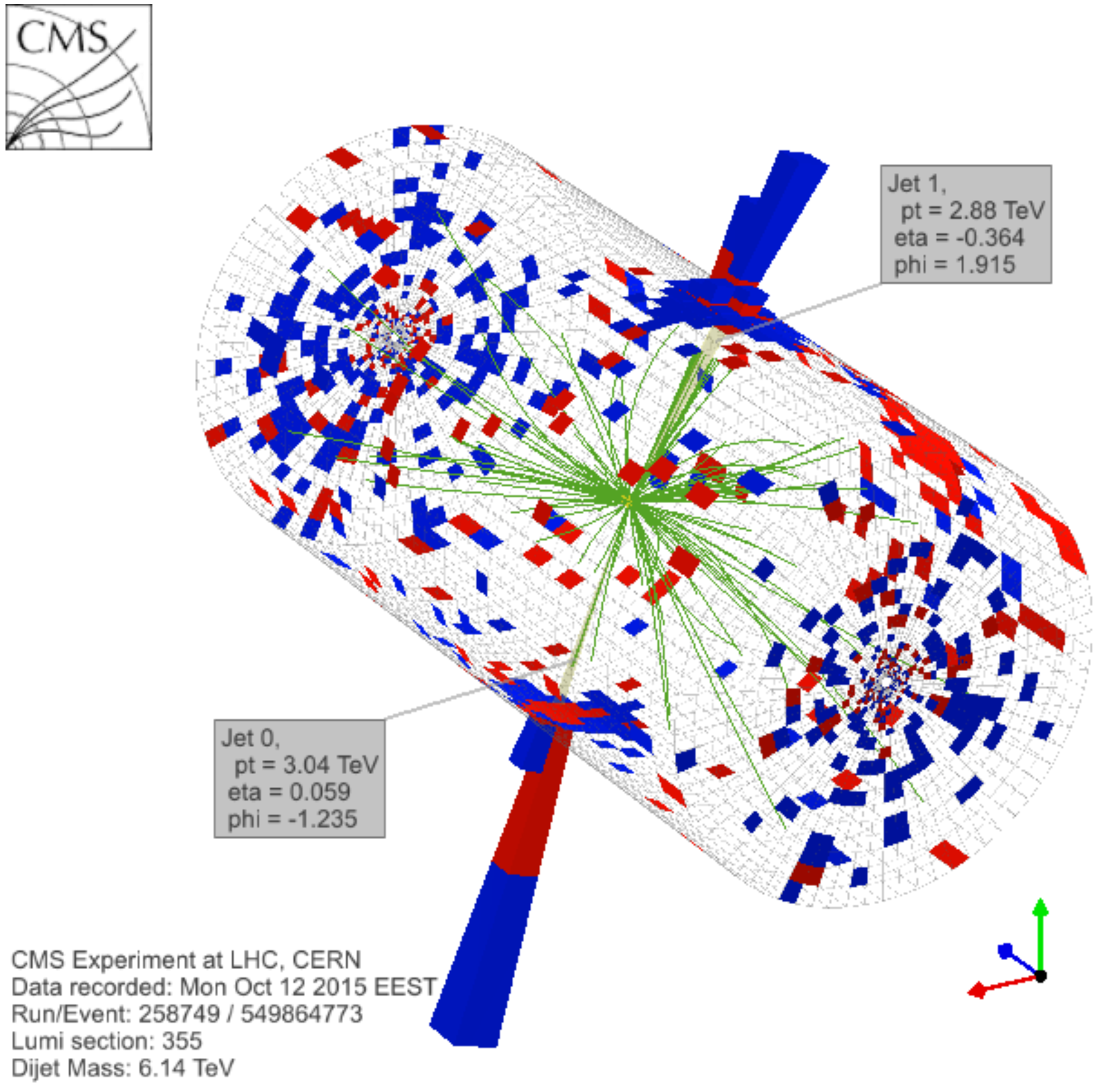

- discriminant: **m_{jj}** and **rapidity difference**
- sensitive to quantum black holes, excited quarks, W'/Z', contact interactions, …
- aim for **model-independent limits**

di-jet resonance spectrum

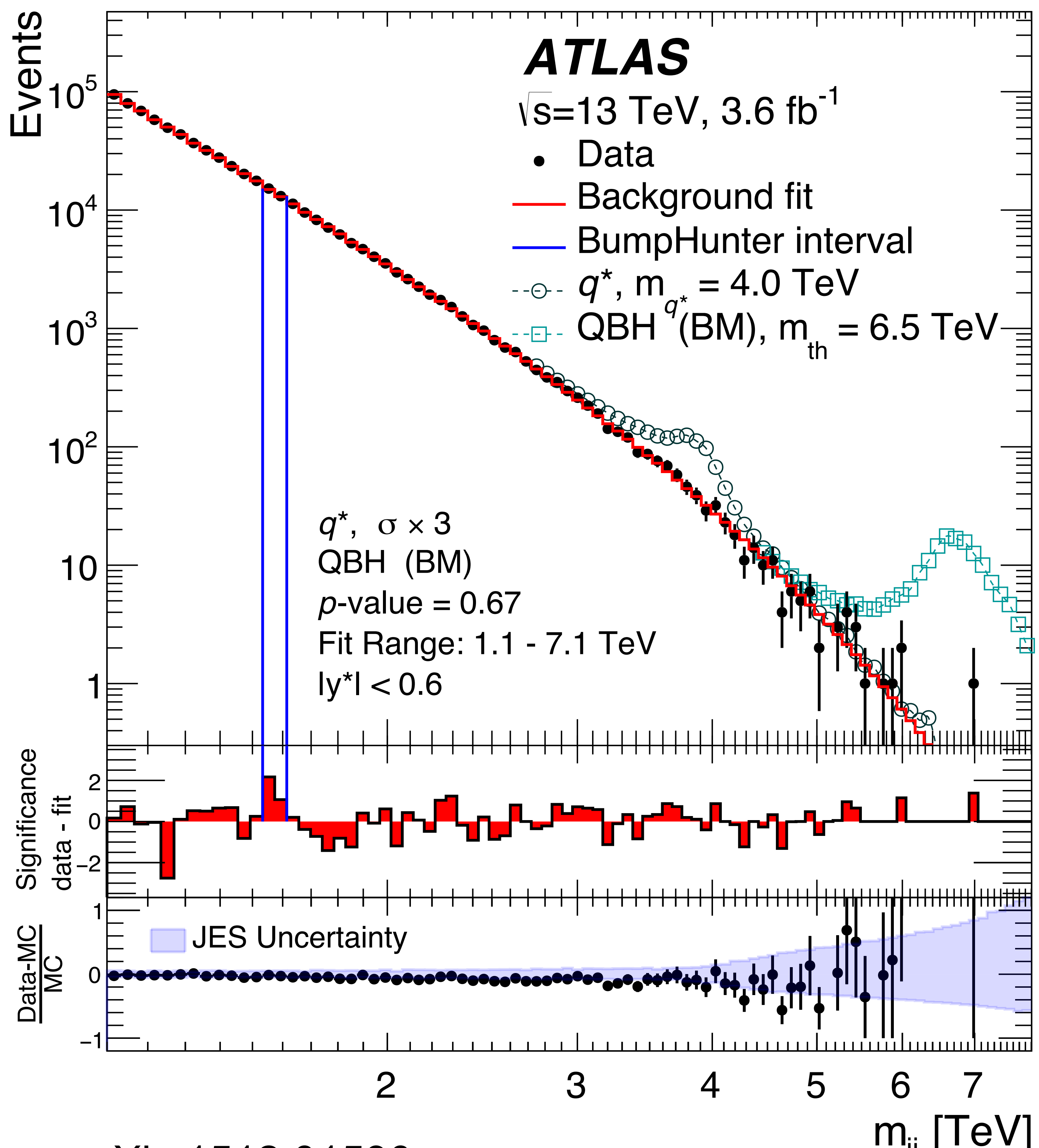

arXiv:1512.01530

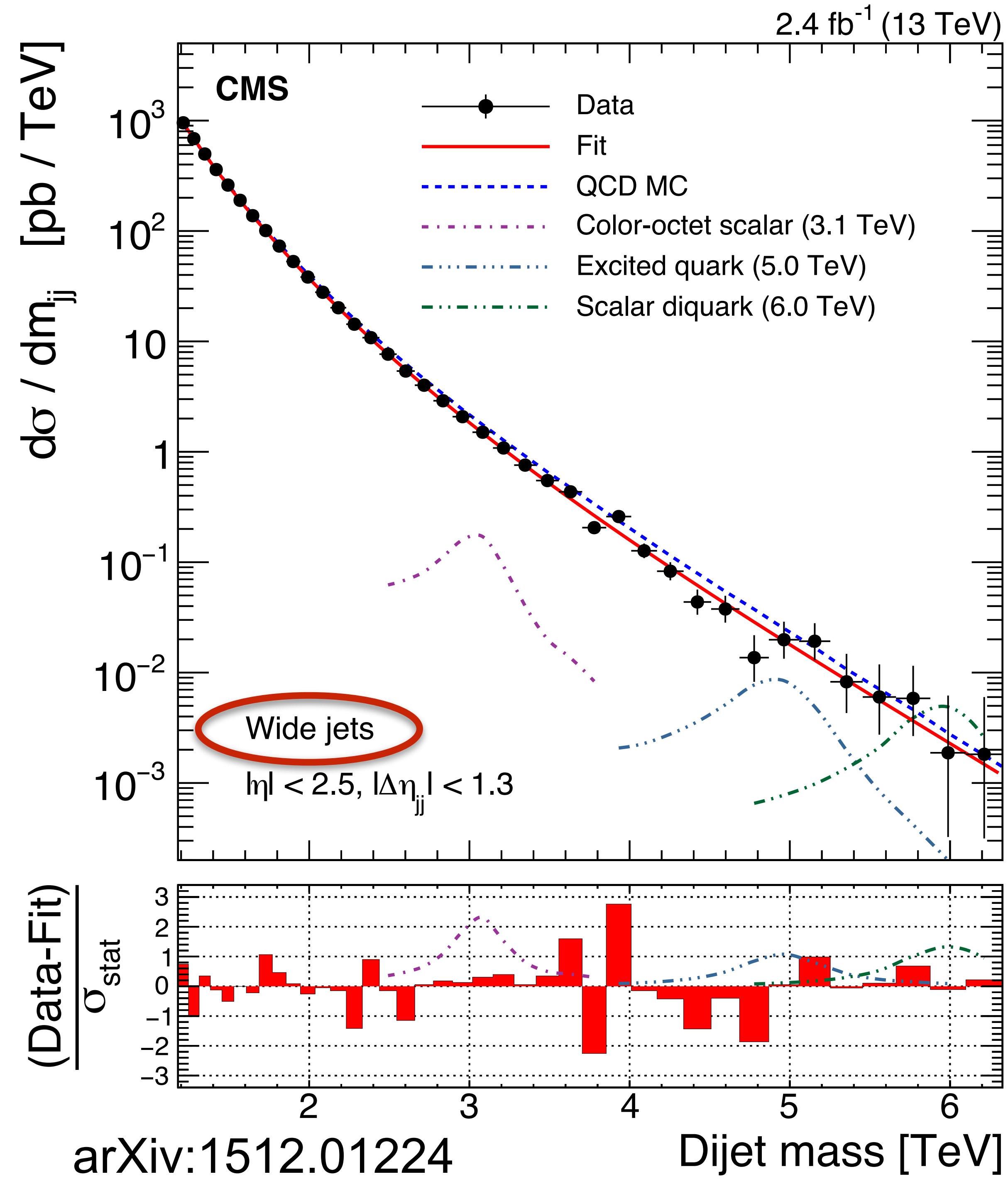

arXiv:1512.01224

no signal found, both analyses significantly extended limits w.r.t. 8 TeV

di-b-jet spectrum

new

- use same background estimation method as di-jet analysis
- single and double b-tag categories sensitive to different signal hypotheses (4th generation b-quark and Z' models)

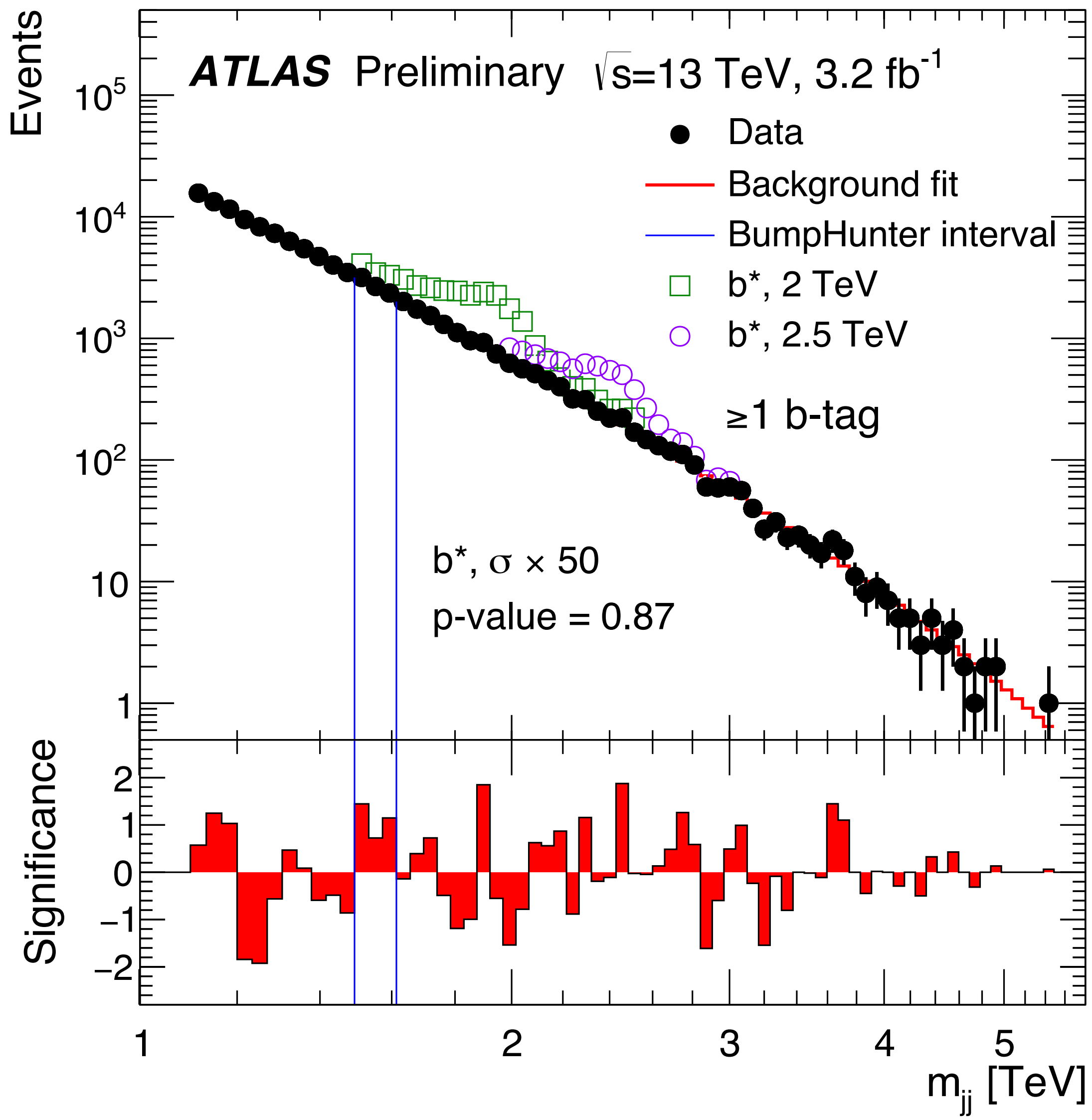

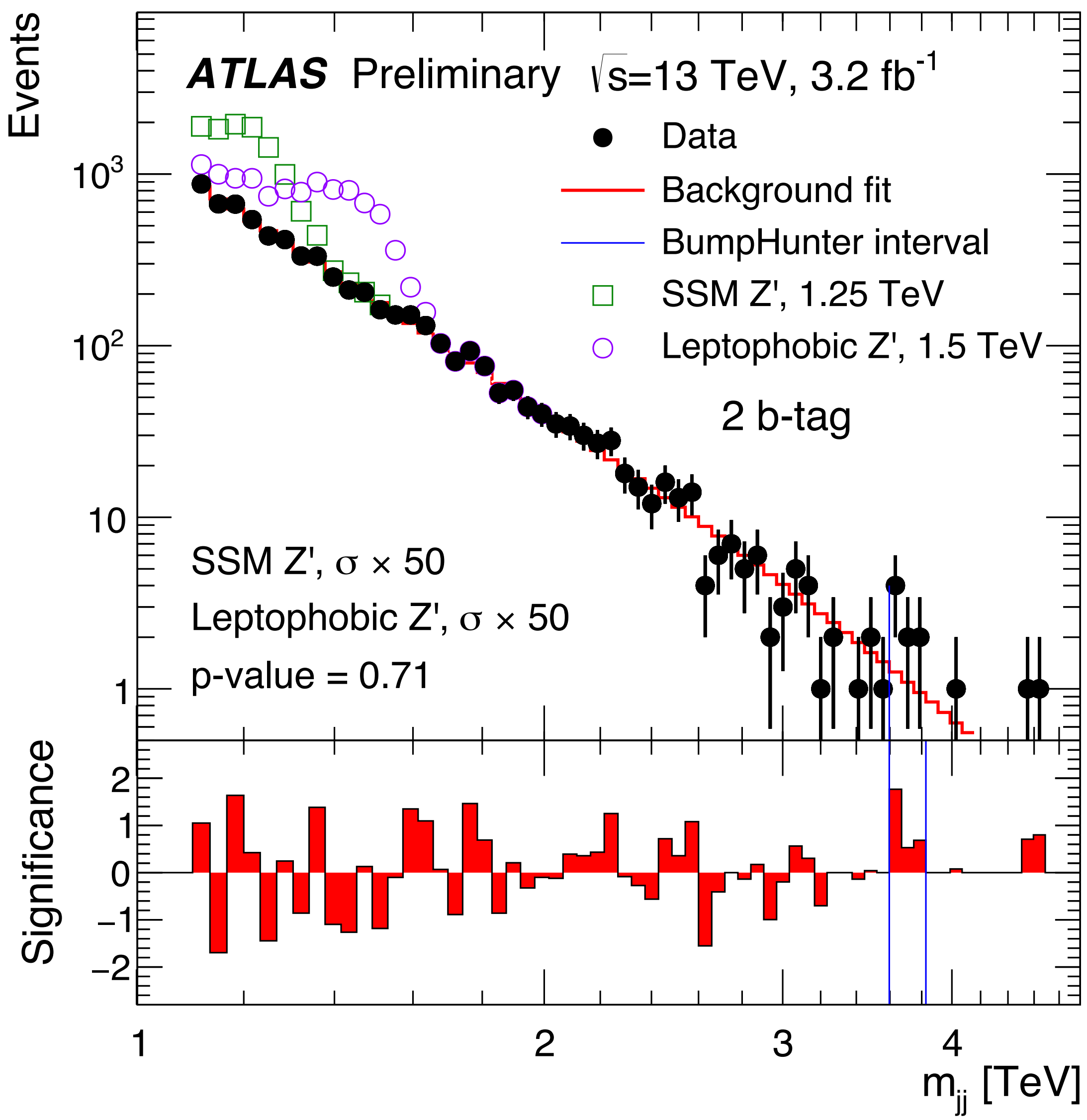

exclude b* in mass range of 1.1-2.1 TeV, not yet sensitive to SSM Z'

University of Zurich[UZH]
Physik-Institut

di-jet angular distribution

distribution expected to be flat for Rutherford scattering

rapidity difference: $\chi = e^{2|y^*|} \sim \frac{1+\cos\theta^*}{1-\cos\theta^*}$

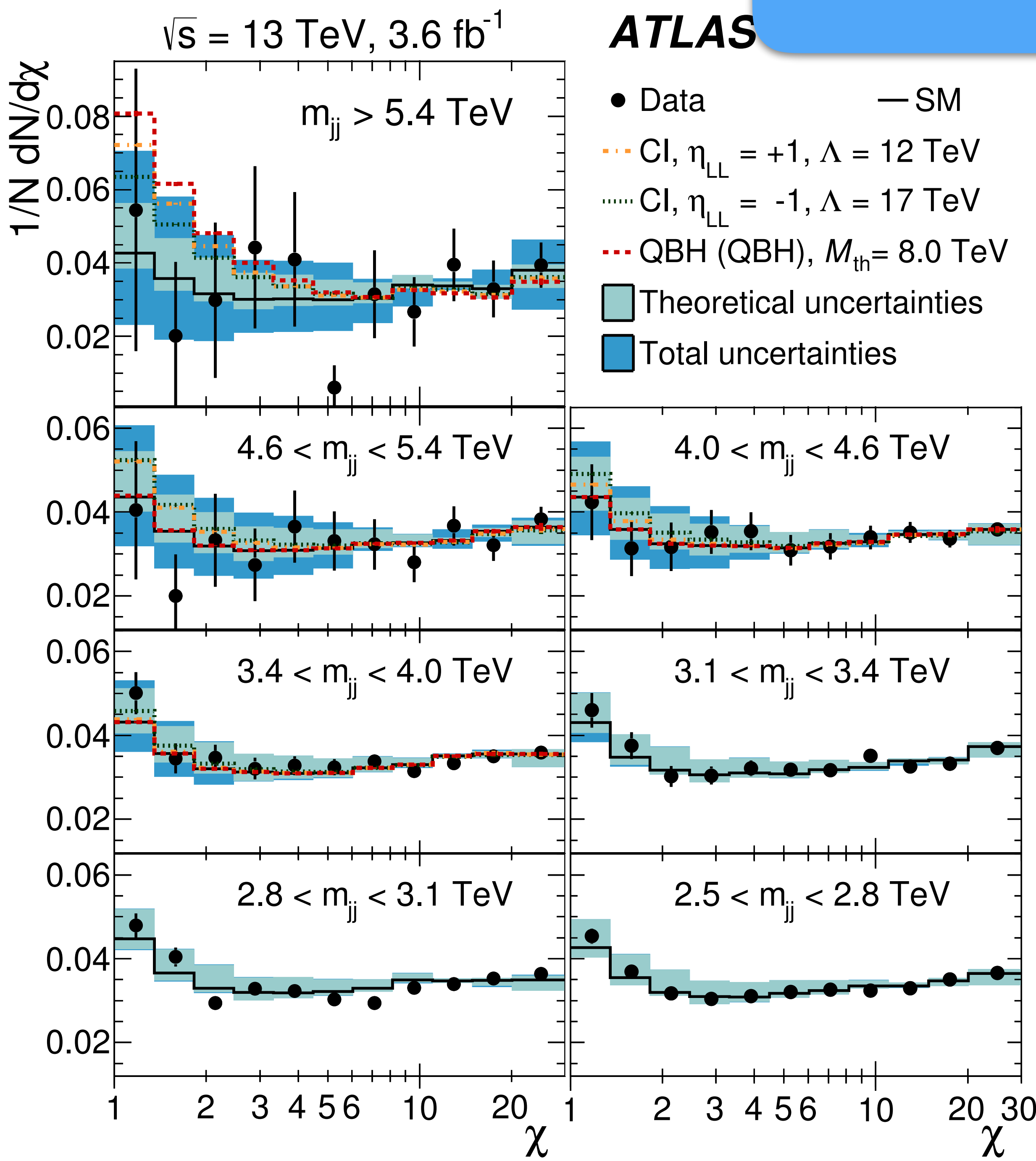

arXiv:1512.01530

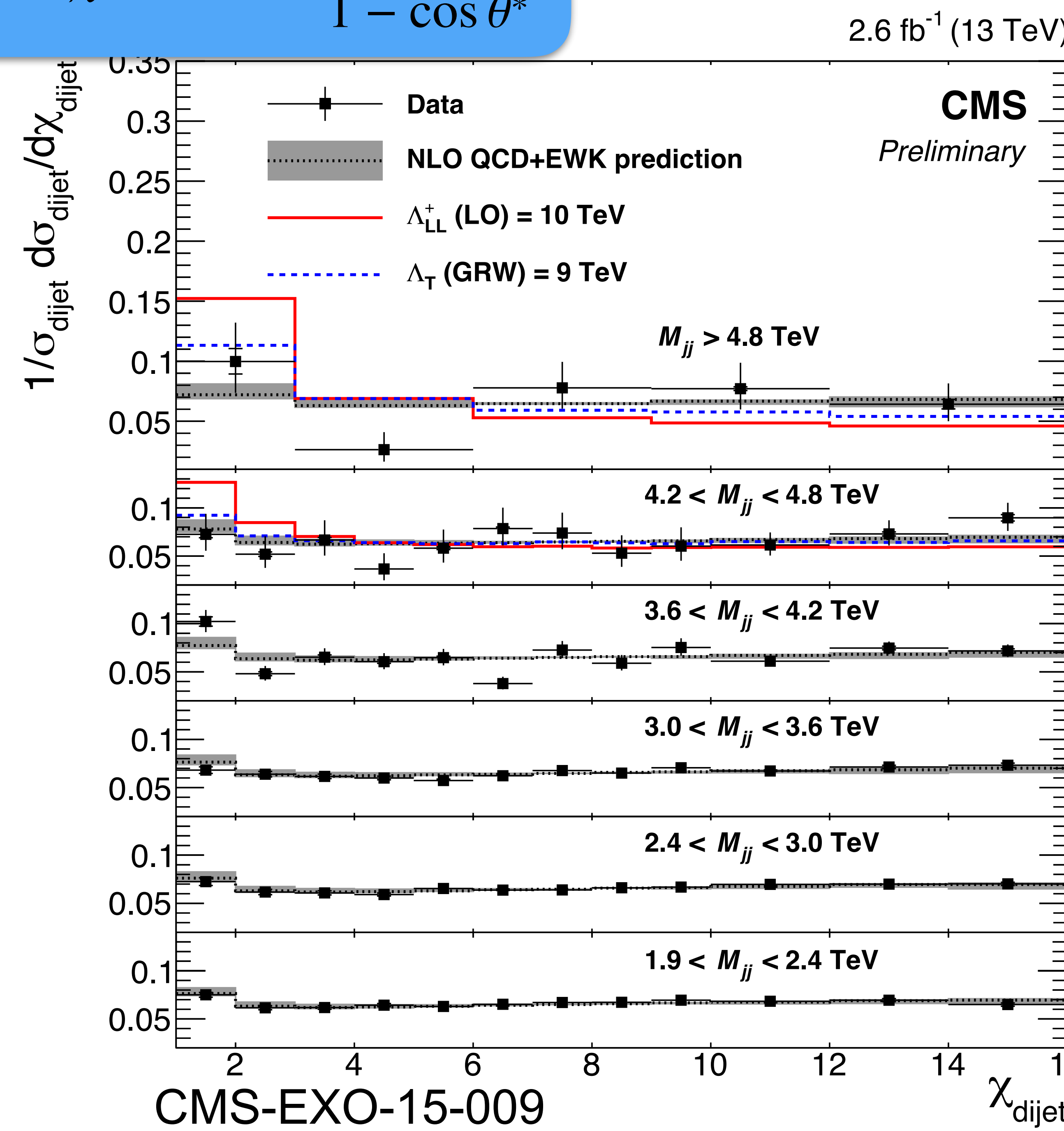

CMS-EXO-15-009

data are compared to NLO predictions (NLOJET++ & EW corrections) in different dijet mass bins

search for strong gravity in H_T spectrum

- search for signs of strong gravity (e.g. thermal black holes) in 3-8 jets final states
- H_T-search: fit low H_T, validate and choose in medium H_T (among 10 functions)
- bootstrap: use incremental datasets to define control regions (6.5 pb^{-1}, 74 pb^{-1}, 440 pb^{-1} and 3.0 fb^{-1})

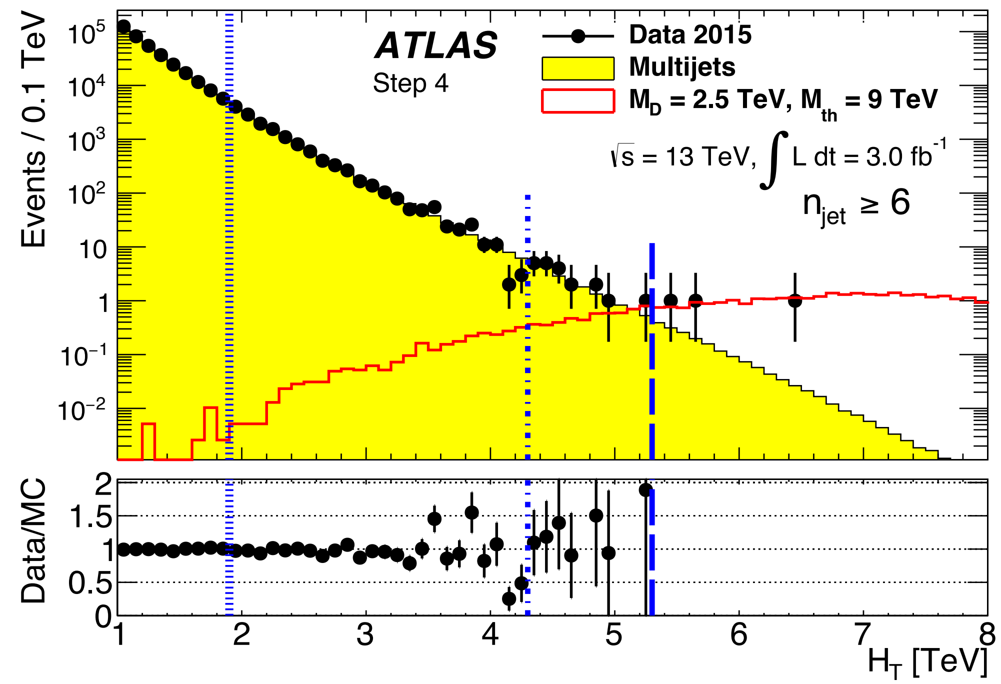

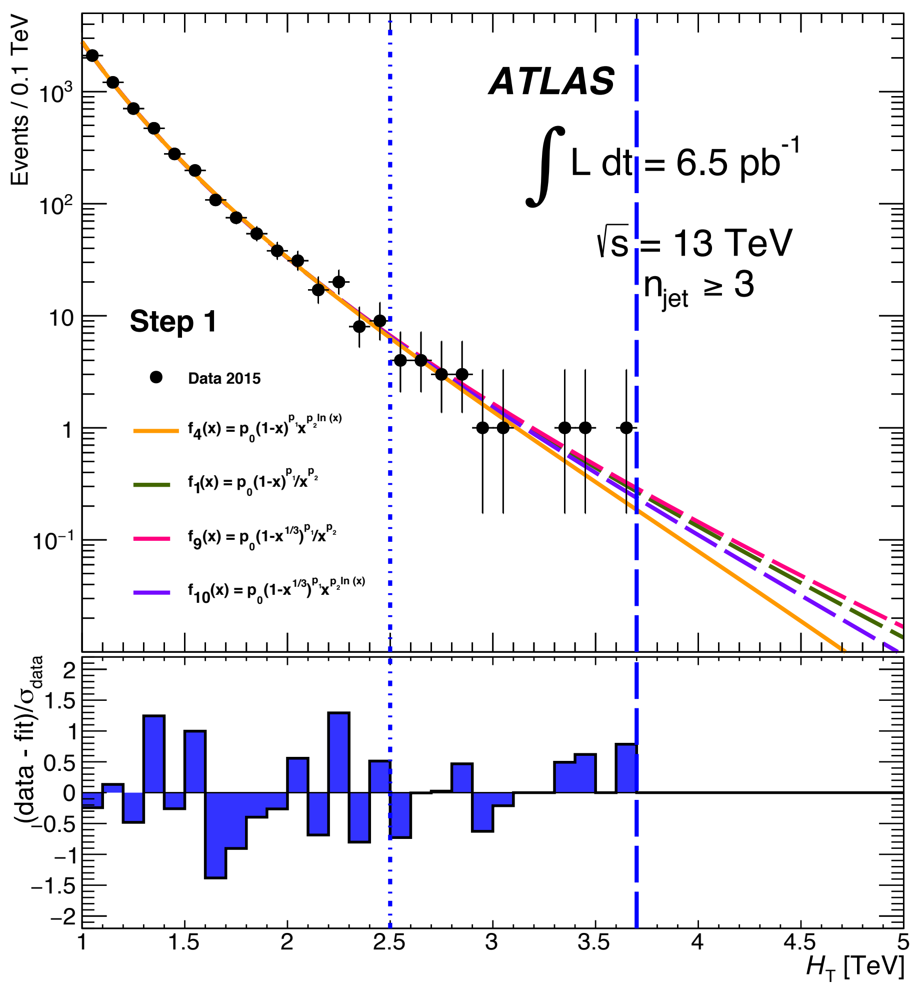

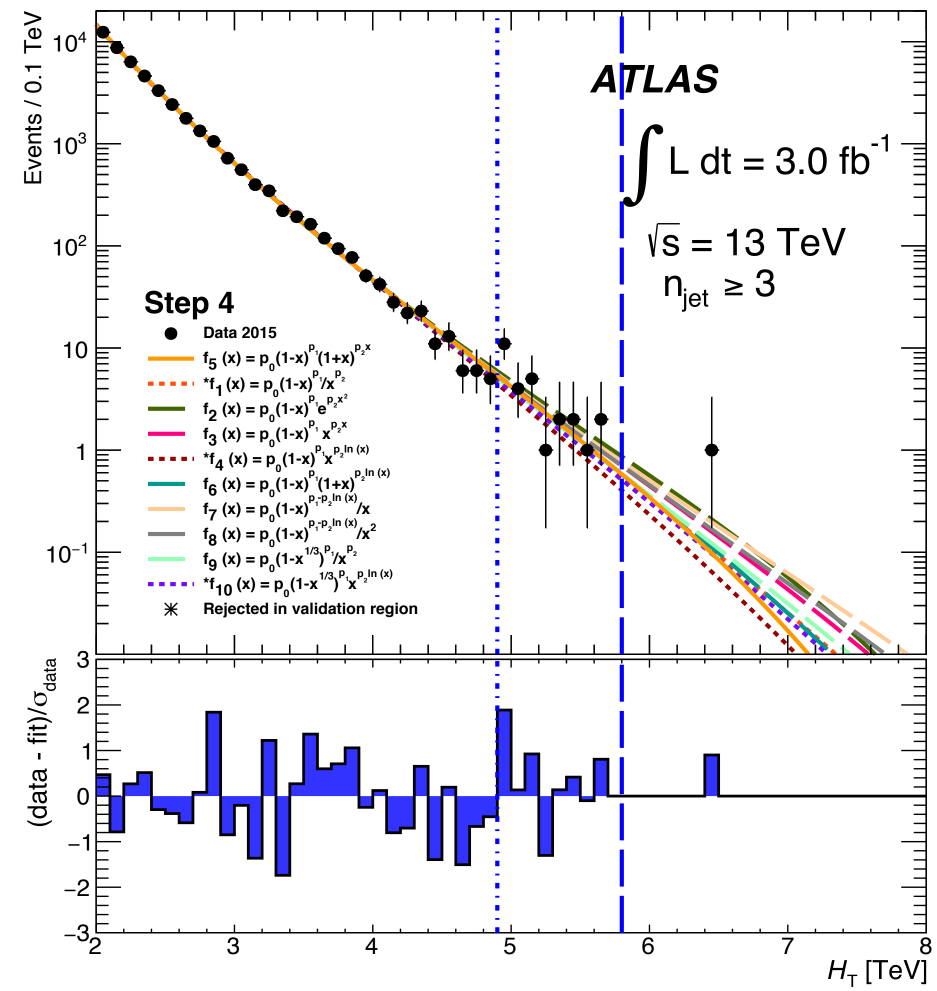

arXiv:1512.02586

search for black holes in S_T spectrum

- select jets, electrons, photons and muons and search in spectrum of scalar sum of their transverse momenta (S_T)
- normalise background fit in low S_T region in different object multiplicity bins (2-10)

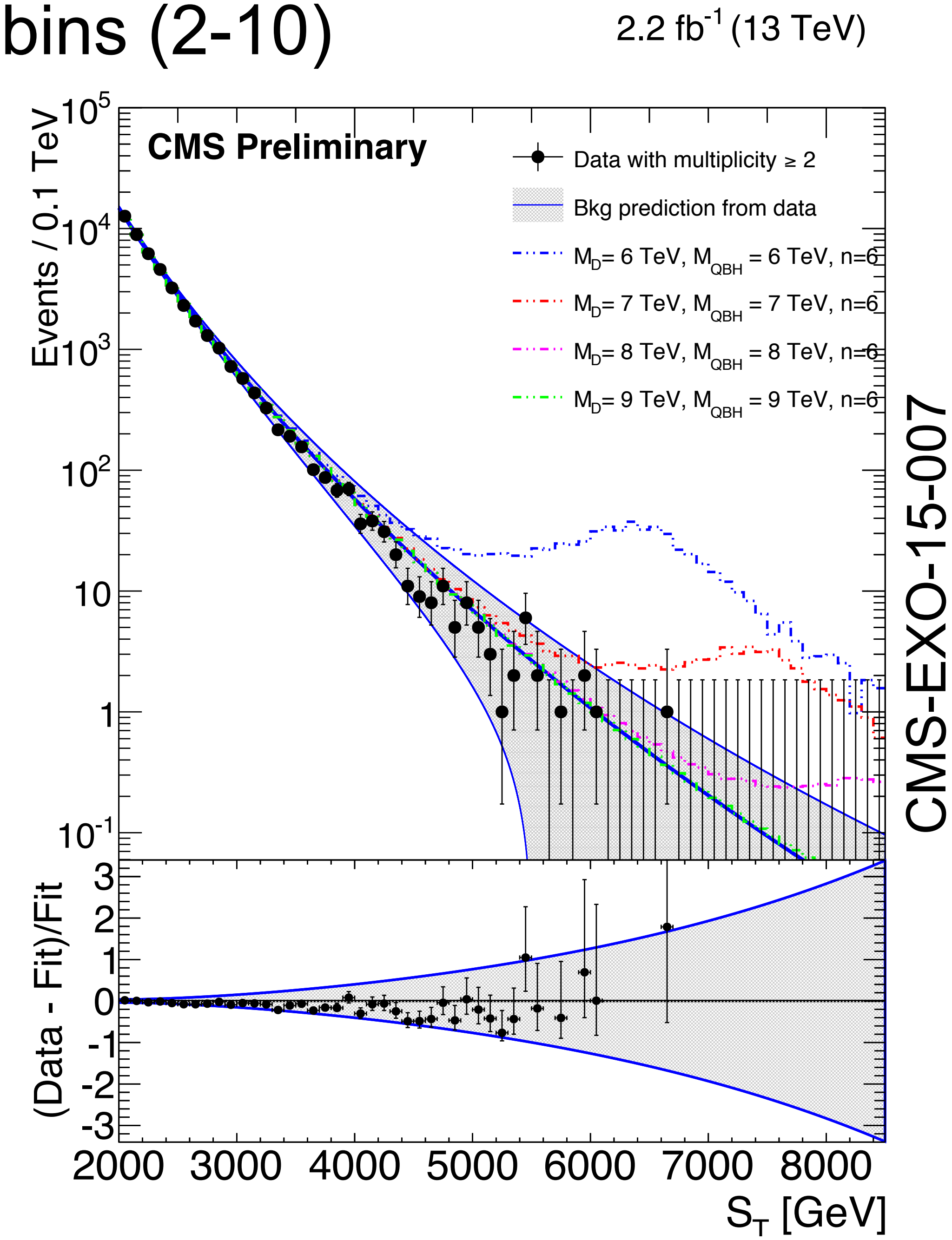

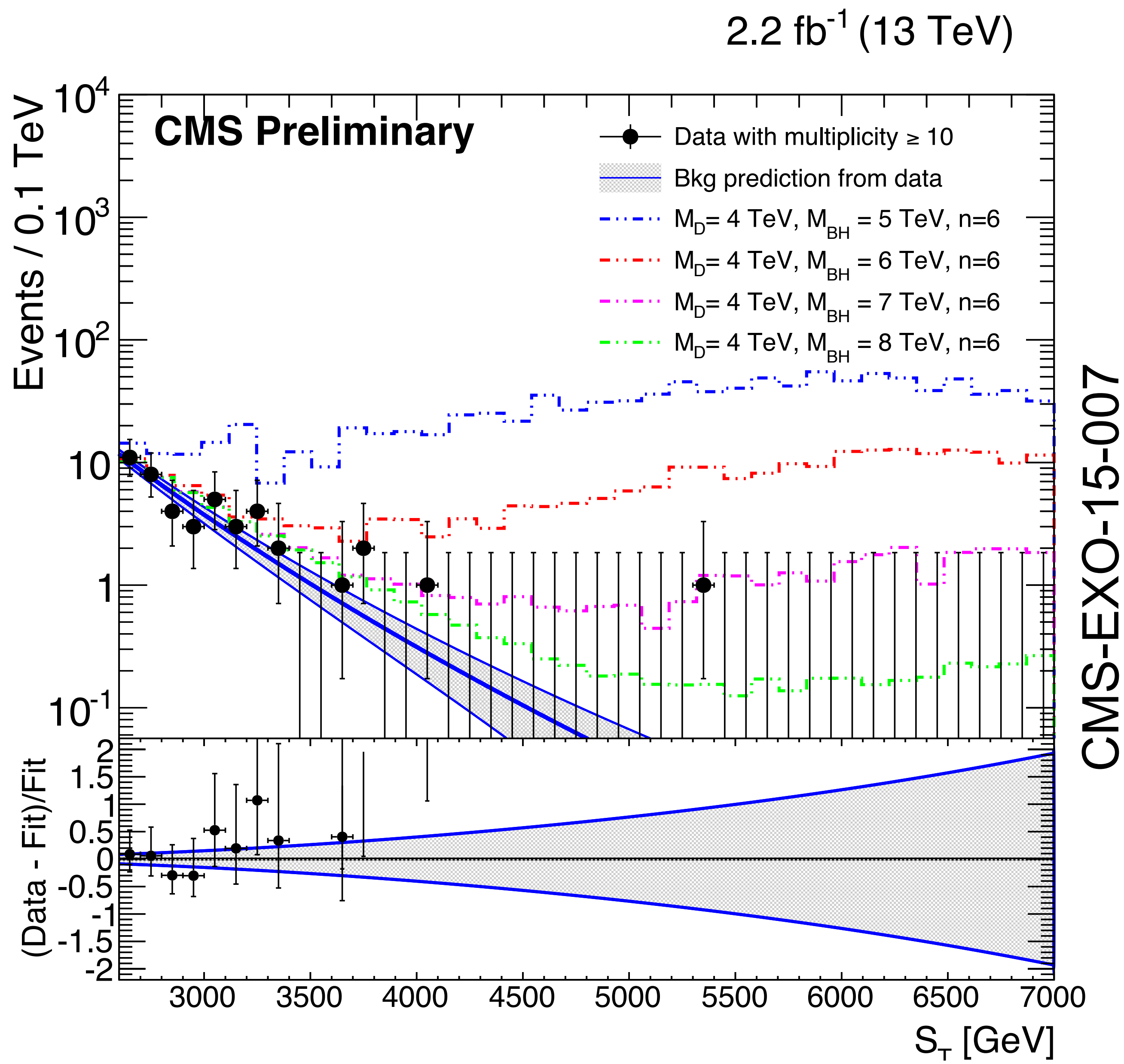

significantly expanded limits w.r.t 8 TeV

jets+leptons final states

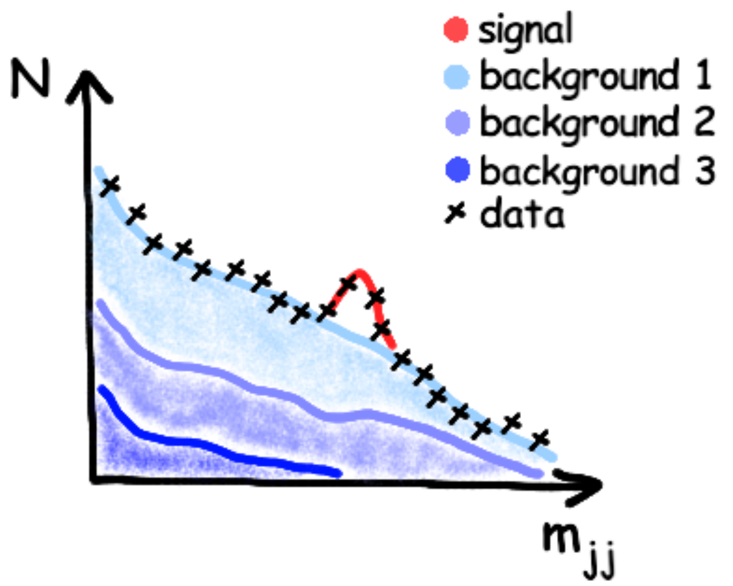

Search for pair production of second generation leptoquarks (ATLAS & CMS)

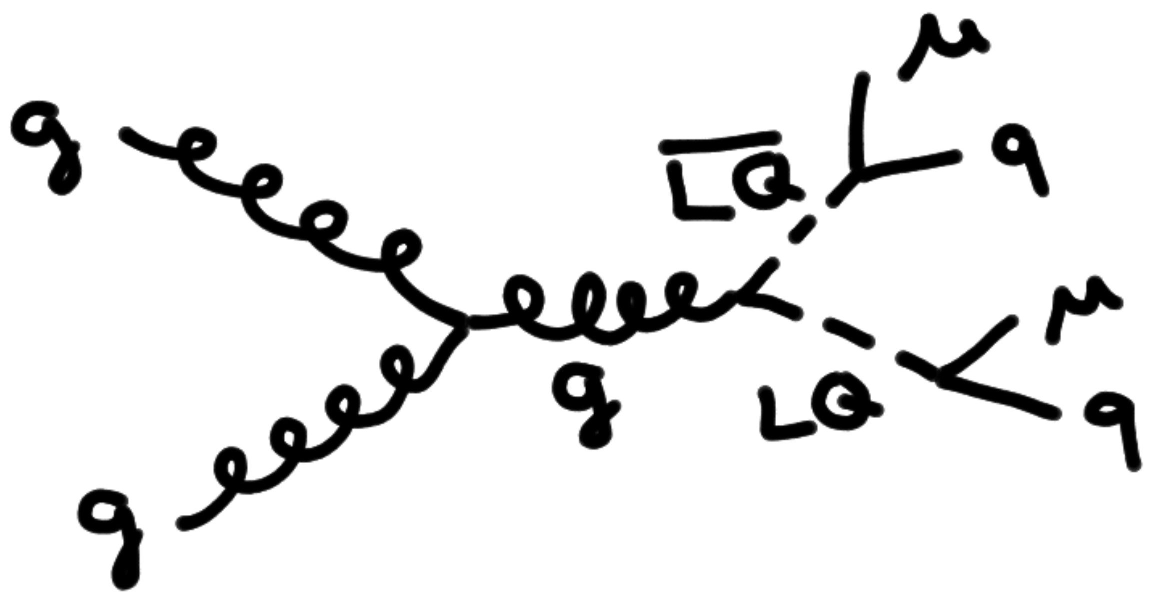

Search for strong gravity in lepton+jets final states (ATLAS)

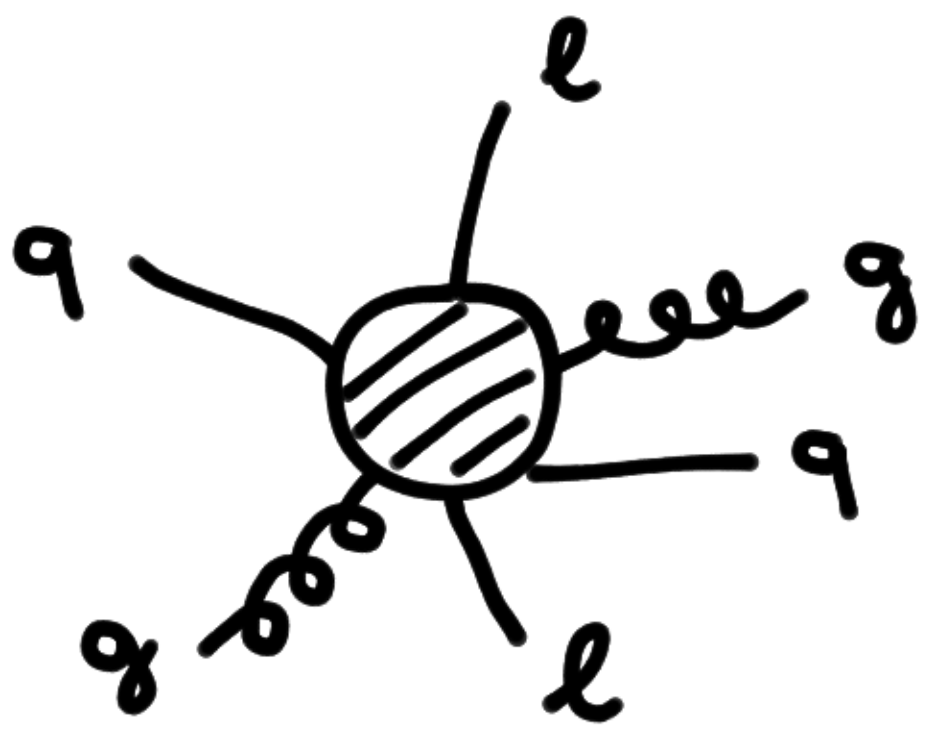

searching for strong gravity in lepton+jets events

new

- **black holes and string balls** expected to decay democratically according to d.o.f. of SM due to energy-momentum tensor coupling
- **enhance signal strength** by selecting **at least one lepton** and suppressing multi-jet background
- select at least three high-p_T objects (jets, muons, electrons)
- search in **scalar p_T-sum** of objects
- confirm background modelling in dedicated control regions (and low sum-p_T)
- perform **combined fit** in all **control regions and signal region**

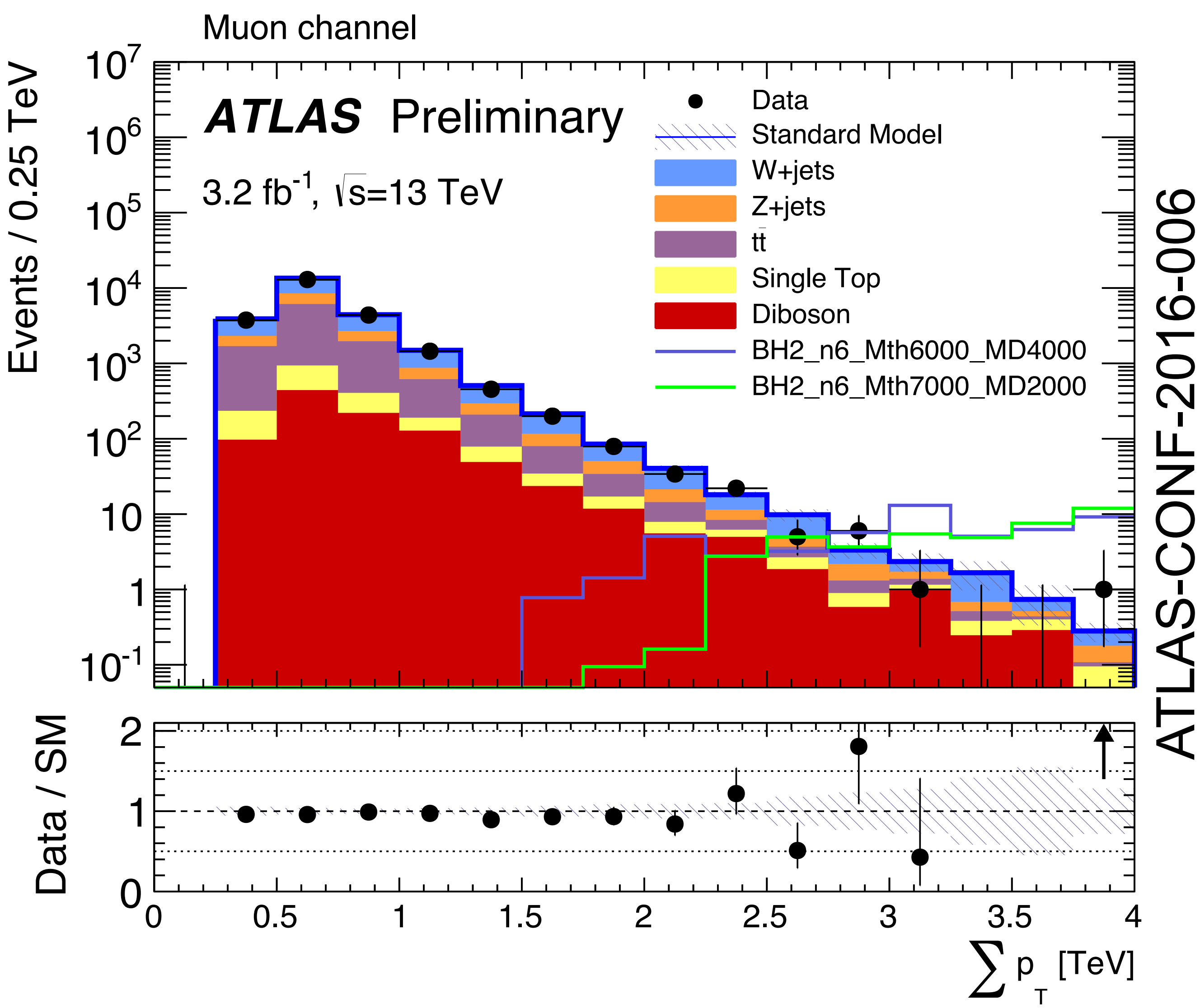

limits w.r.t. 8 TeV improved by 2-3 TeV depending on model parameters

search for pair production of second generation leptoquarks

University of Zurich[UZH]
Physik-Institut

new

- leptoquarks (hypothetical particles containing both baryon and lepton numbers) expected to be produced in pairs at the LHC
- **2 muon + 2 jets final state**
  - veto Z-window
  - apply cuts on **sum of p_T** (S_T) and **min($m_{\mu j}$)** to minimise LQ-LQ mass difference
  - optimised for each signal mass hypothesis (200-1500 GeV)
- dominant **background** processes (Drell-Yan, tt) **estimated in sidebands**
- count events in each mass window
- exclude leptoquarks with masses < 1150 GeV (assuming 100% BR to lepton + quark)

650 & 900 GeV hypothesis

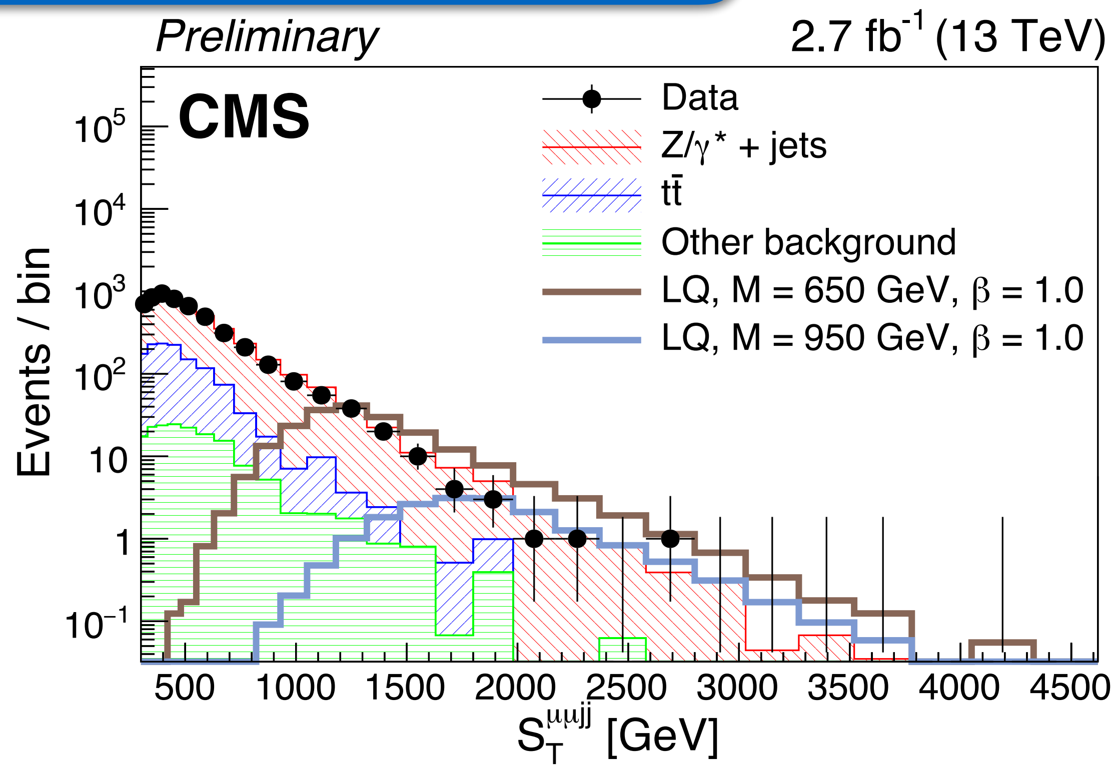

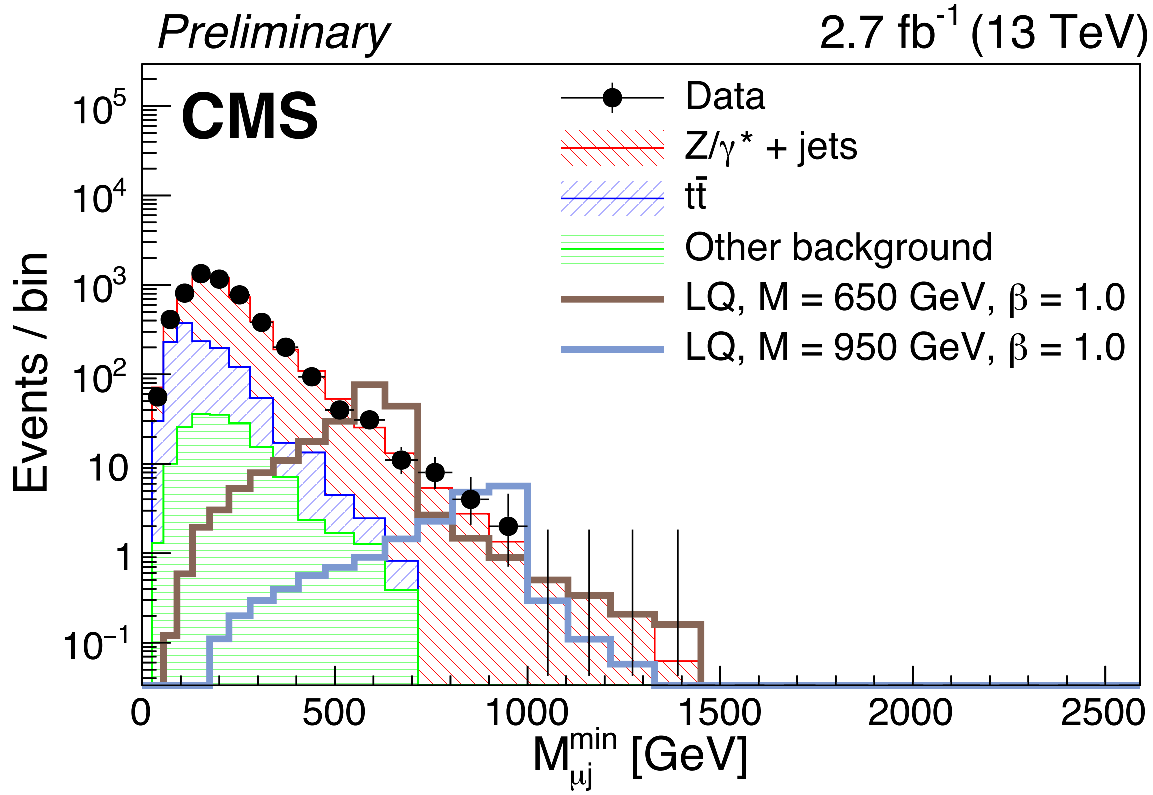

CMS-EXO-16-007

conclusions and outlook

- no matter if the di-photon bump is real or not, there are **loads of reasons** to **search for new physics in multi-jet final states**
- largely thanks to **parton luminosity scaling**, previously obtained **limits** have been **significantly improved** with 13 TeV data using only a fraction of the data statistics compared to the 8 TeV run
- 2016, commencing the luminosity ramp-up at 13 TeV, will be another exciting year at the LHC

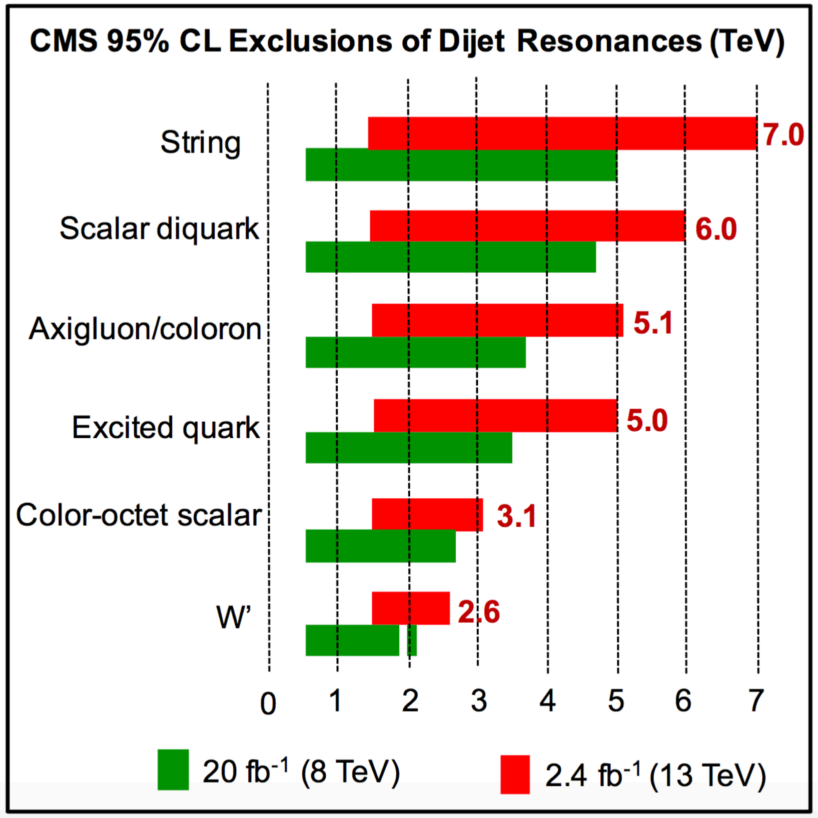

arXiv:1512.01224

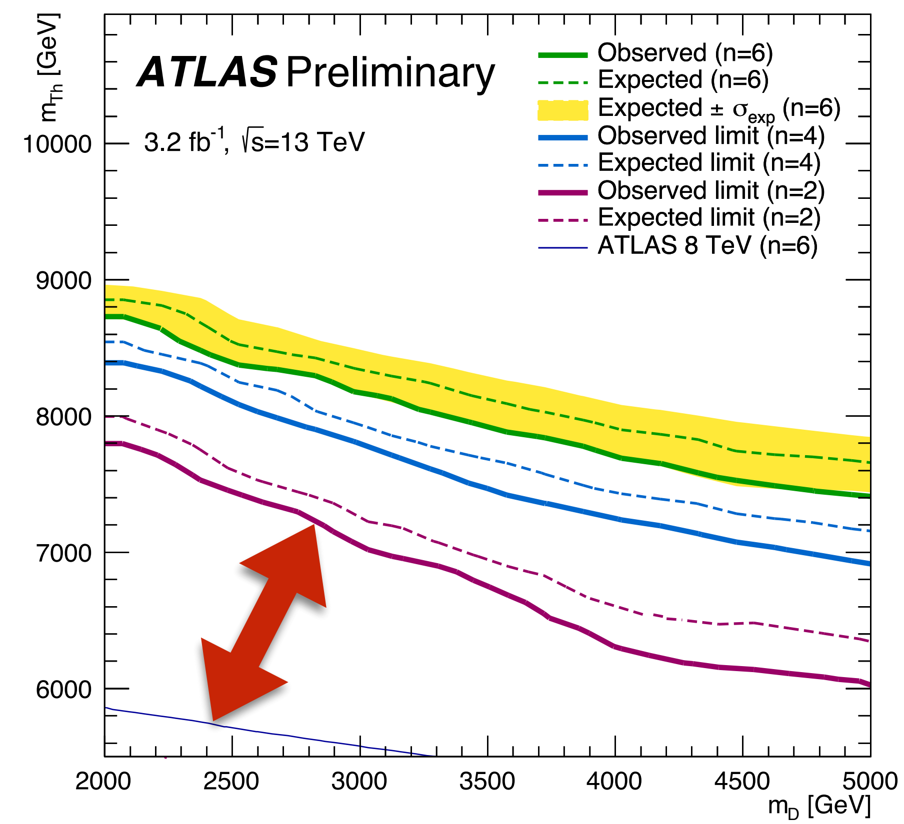

ATLAS-CONF-2016-006

everybody back-up

backup slides

- CMS di-jet search: http://cms-results.web.cern.ch/cms-results/public-results/publications/EXO-15-001/
- ATLAS di-jet and angular distribution search: https://atlas.web.cern.ch/Atlas/GROUPS/PHYSICS/PAPERS/EXOT-2015-02/
- CMS angular distribution search: http://cms-results.web.cern.ch/cms-results/public-results/preliminary-results/EXO-15-009/
- ATLAS di-jet search with b-jets: not yet available (EXOT-2015-22)
- CMS search for black holes: http://cms-results.web.cern.ch/cms-results/public-results/preliminary-results/EXO-15-007/
- ATLAS search for strong gravity in multi-jets: https://atlas.web.cern.ch/Atlas/GROUPS/PHYSICS/PAPERS/EXOT-2015-09/
- CMS search for leptoquarks: not yet available (EXO-16-007)
- ATLAS gravity search in l+jets: https://atlas.web.cern.ch/Atlas/GROUPS/PHYSICS/CONFNOTES/ATLAS-CONF-2016-006/

how to lower thresholds?

- parked (not promptly reconstructed) data written to tape
- dedicated data scouting analyses

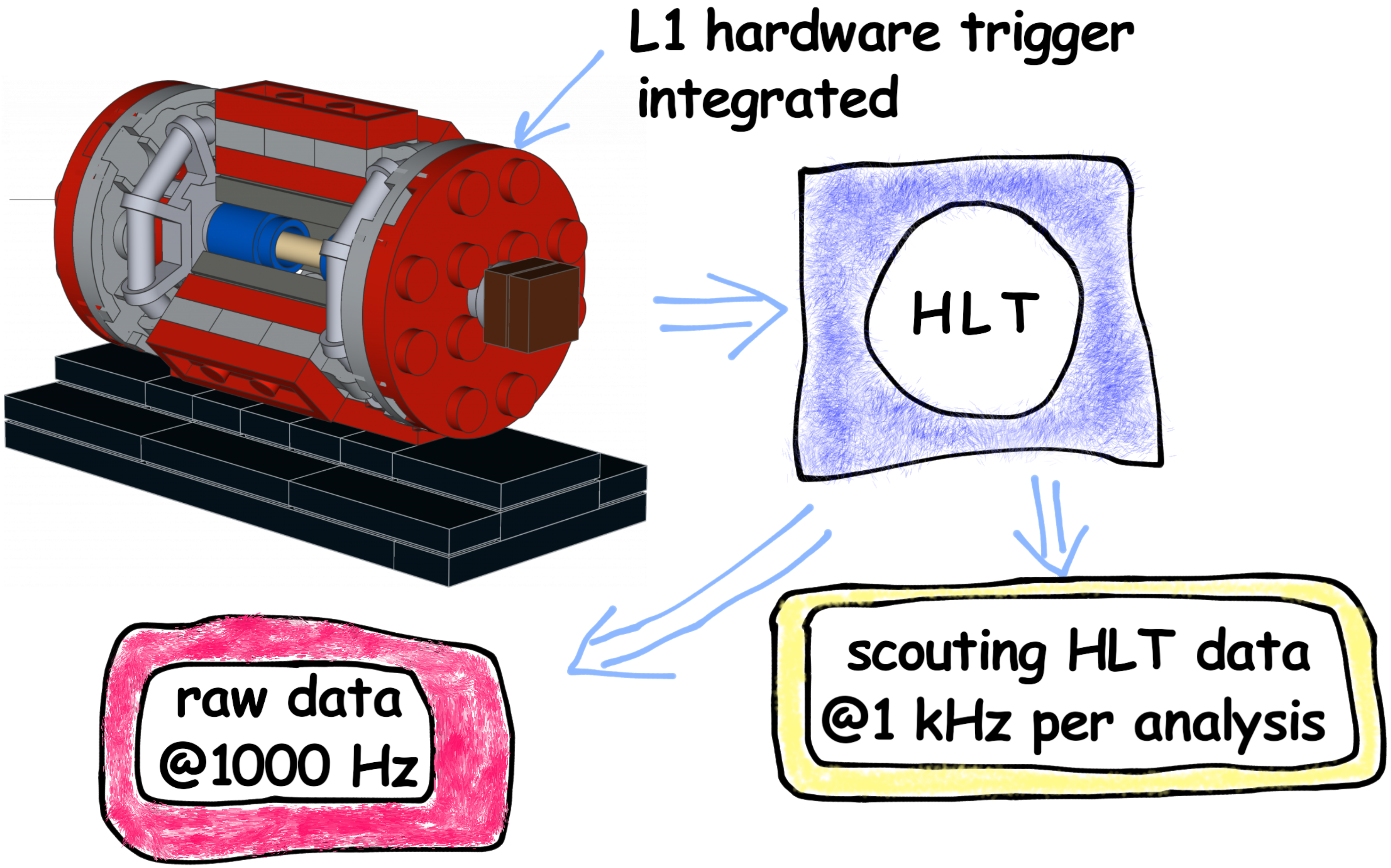

ATLAS dijet resonance search

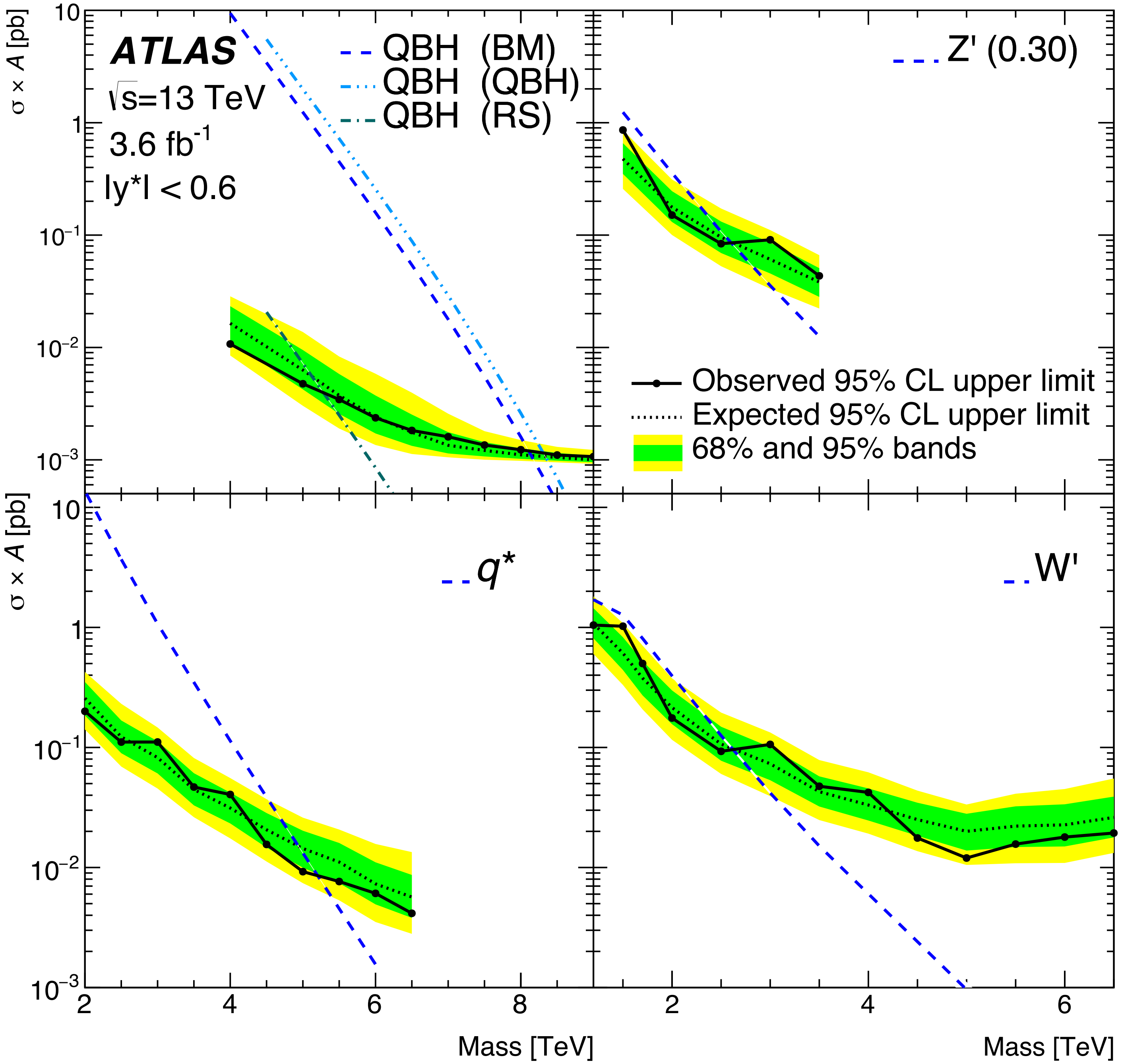

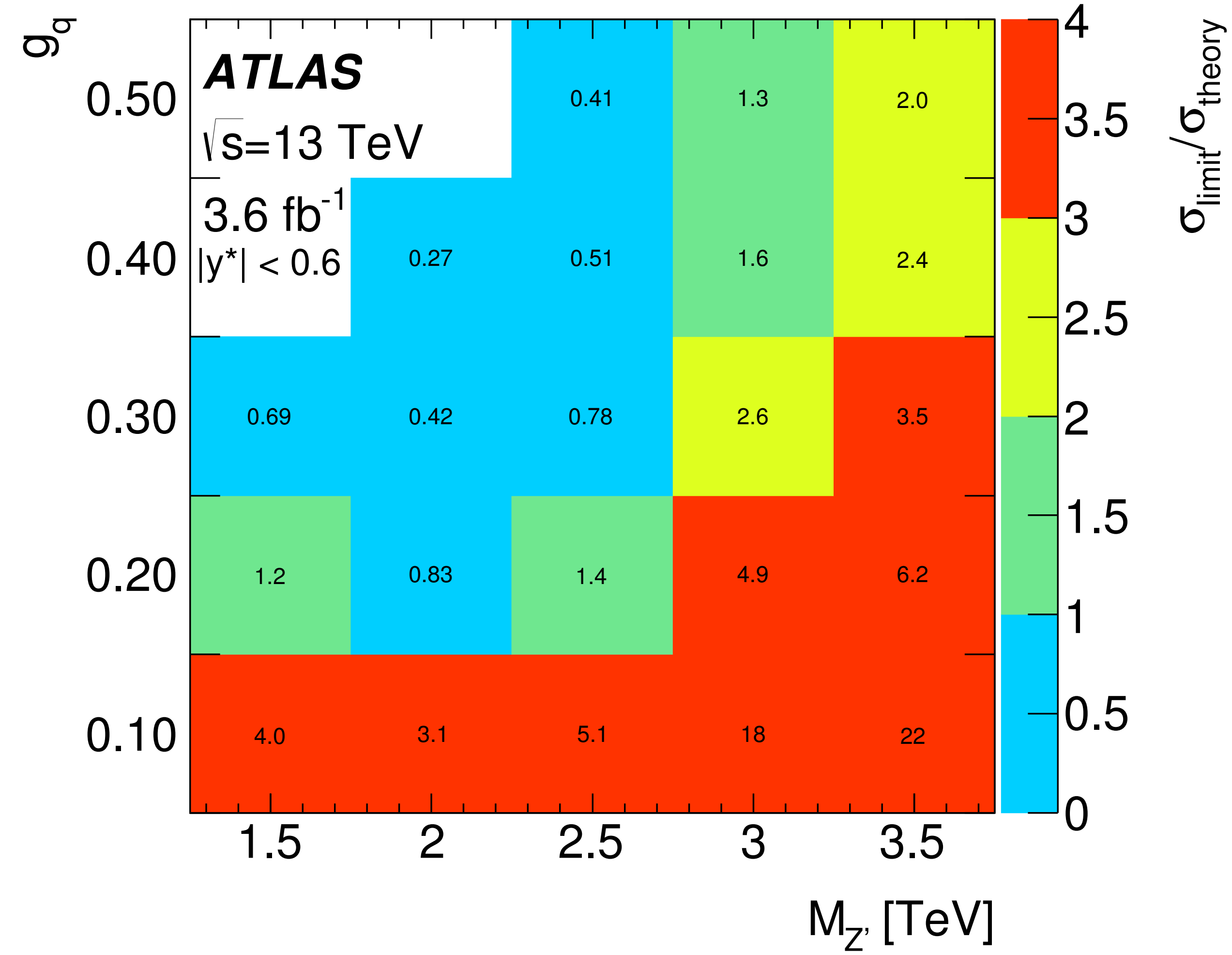

ATLAS dijet resonance search

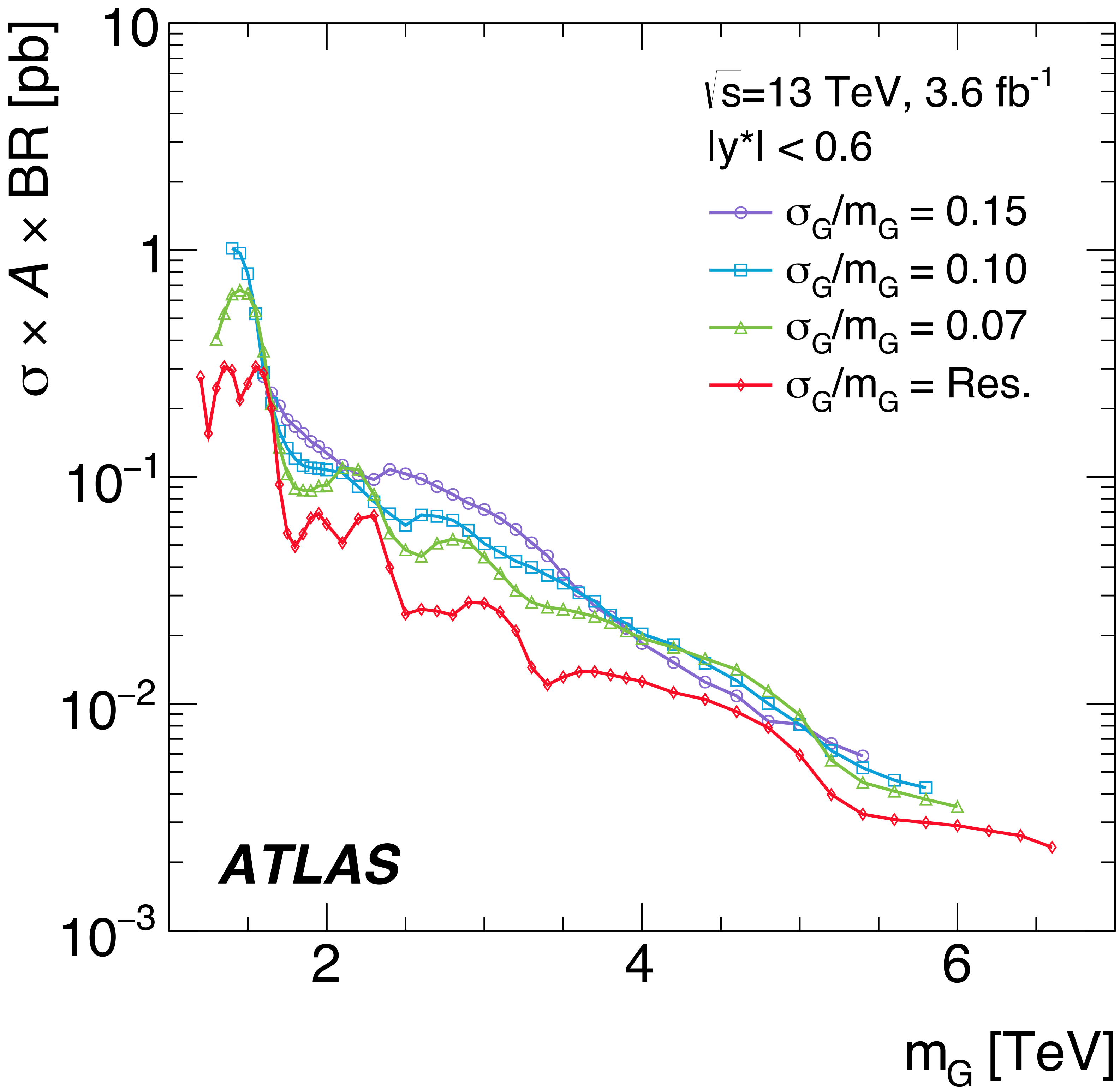

CMS dijet resonance search

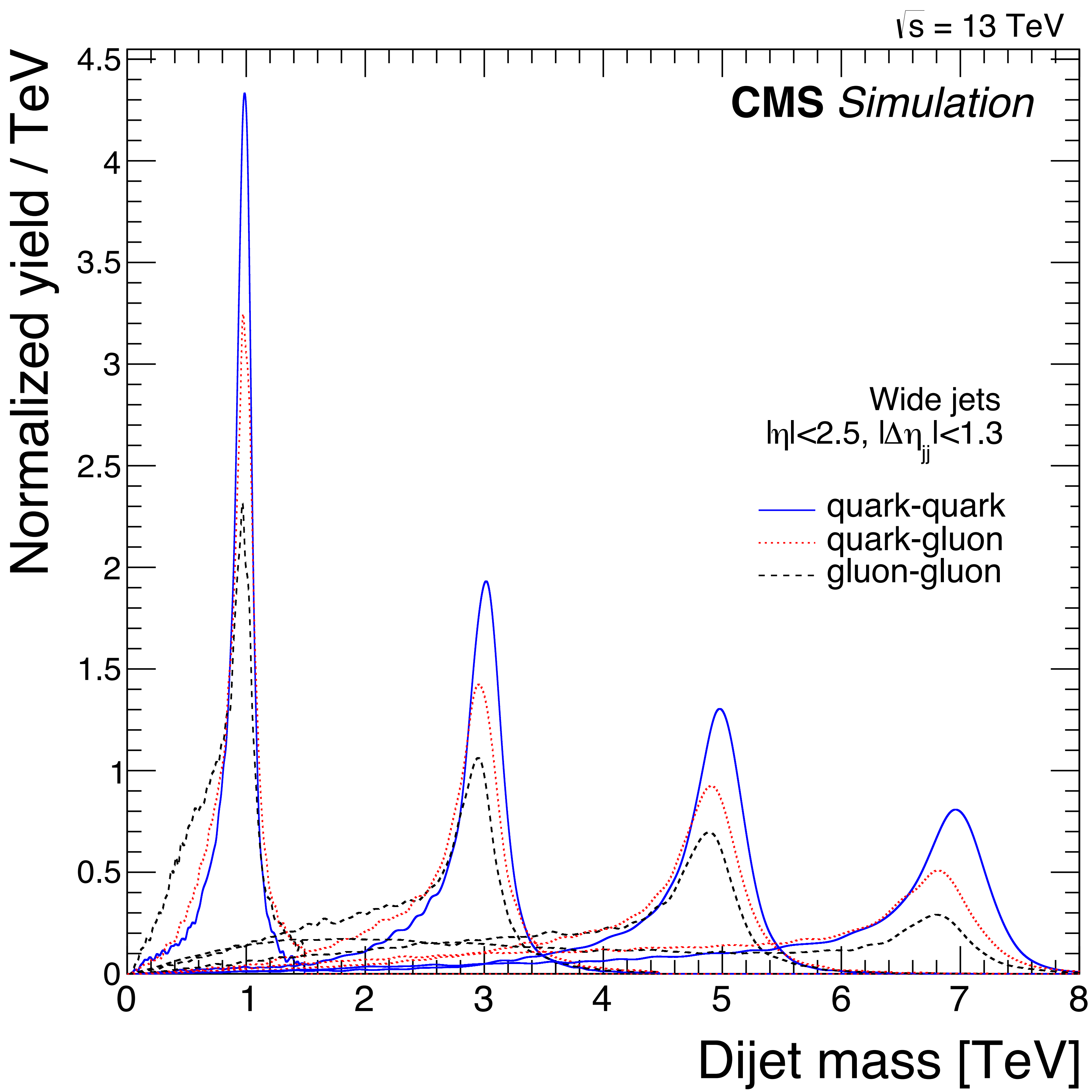

CMS dijet resonance search

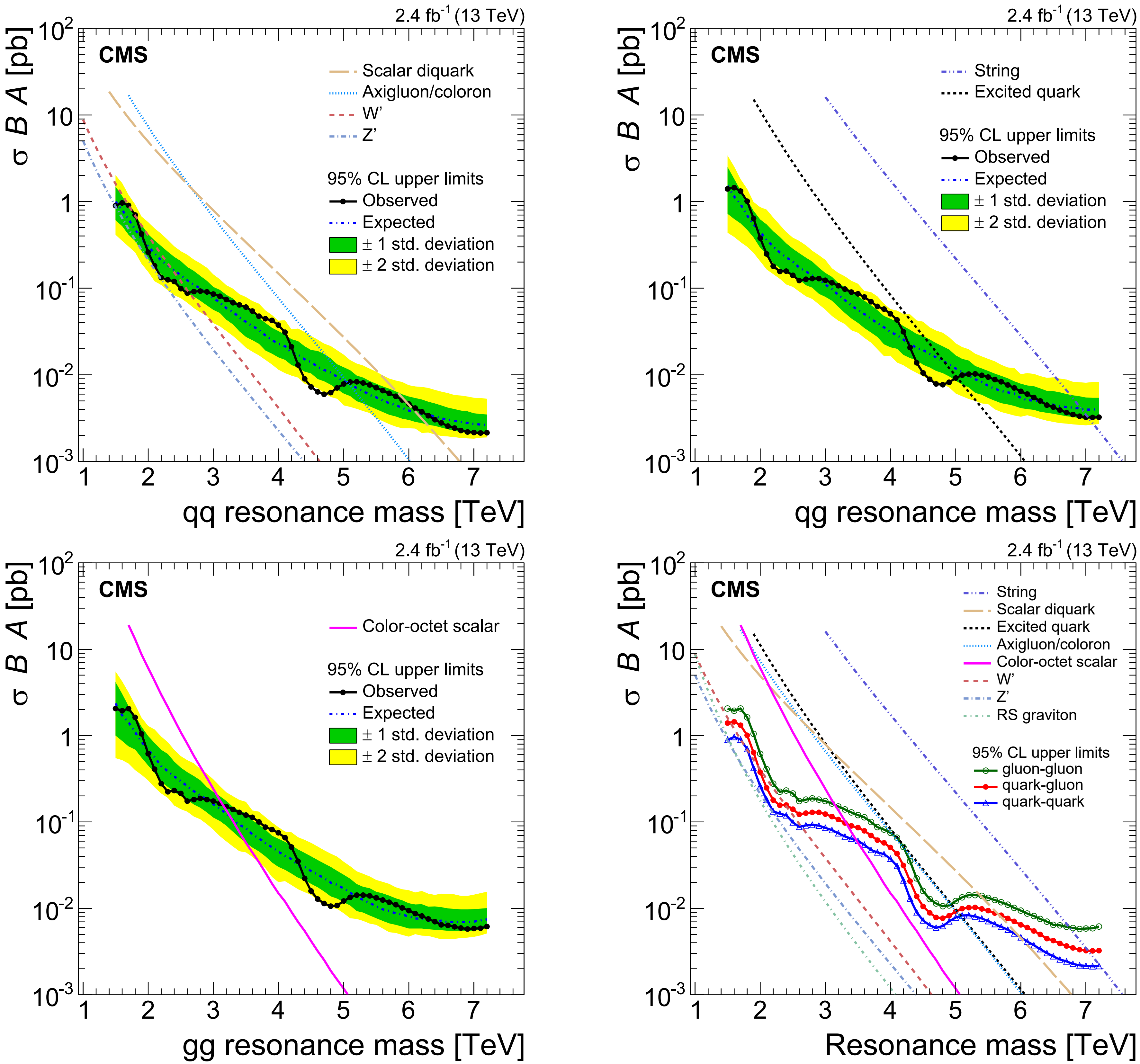

CMS dijet resonance search

Model	Final State	Obs. Mass Limit [TeV]	Exp. Mass Limit [TeV]
String	qg	7.0	6.9
Scalar diquark	qq	6.0	6.1
Axigluon/coloron	$q\bar{q}$	5.1	5.1
Excited quark (q^*)	qg	5.0	4.8
Color-octet scalar	gg	3.1	3.3
Heavy W (W')	$q\bar{q}$	2.6	2.3

ATLAS dijet angular search

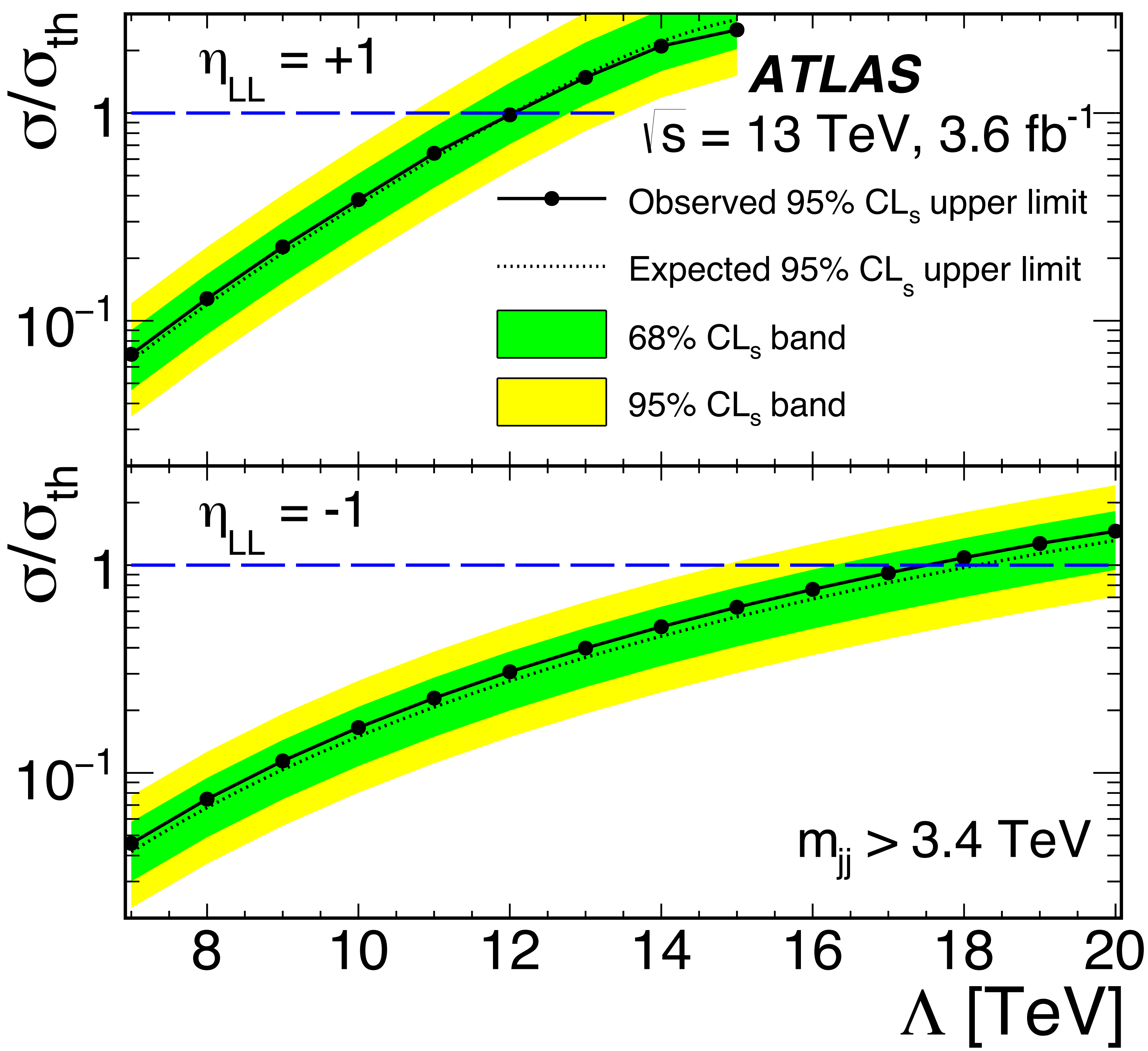

CMS dijet angular search

Table 1: Summary of leading experimental and theoretical uncertainties on the normalized χ_{dijet} distributions. While in the statistical analysis each uncertainty is represented by a change of the χ_{dijet} distribution correlated among all χ_{dijet} bins, this table summarizes each uncertainty by a representative number to demonstrate the relative contributions. For the lowest and highest dijet mass bins, the relative shift of the lowest χ_{dijet} bin from its nominal value is quoted. In the highest dijet mass bin, the dominant experimental contribution is the statistical uncertainty while the dominant theoretical contribution is the scale uncertainty.

Uncertainty	$1.9 < M_{jj} < 2.4$ TeV	$M_{jj} > 4.8$ TeV
Statistical	1.6%	24%
Jet energy scale	3.0%	9.5%
Jet energy resolution (core)	<1%	2.0%
Jet energy resolution (tails)	<1%	2.5%
Unfolding, MC modeling	<1%	<1%
Unfolding, detector simulation	1.0%	3.0%
Pileup	<1%	<1%
Total experimental	9.7%	26%
NLO scale (6 variations of μ_R and μ_F)	$^{+7.9\%}_{-2.8\%}$	$^{+13\%}_{-4.9\%}$
PDF (CT14 eigenvectors)	0.15%	0.4%
Non-perturbative corrections (Pythia8 vs. Herwig++)	<1%	<1%
Total theoretical	7.9%	13%

Table 2: Observed and expected exclusion limits at 95% CL for various CI and extra dimension models.

Compositeness model	Observed lower limit (TeV)	Expected lower limit (TeV)
$\Lambda^{+}_{LL/RR}$ (LO)	12.1	12.0 ± 1.1
$\Lambda^{-}_{LL/RR}$ (LO)	16.3	15.3 ± 2.4
ADD Λ_T (GRW)	9.1	9.0 ± 0.7
ADD M_S (HLZ) $n_{ED} = 2$	9.7	9.6 ± 0.7
ADD M_S (HLZ) $n_{ED} = 3$	10.8	10.7 ± 0.8
ADD M_S (HLZ) $n_{ED} = 4$	9.2	9.0 ± 0.7
ADD M_S (HLZ) $n_{ED} = 5$	8.3	8.1 ± 0.6
ADD M_S (HLZ) $n_{ED} = 6$	7.7	7.6 ± 0.6

ATLAS search for strong gravity in multi-jets

University of Zurich[UZH]

Physik-Institut

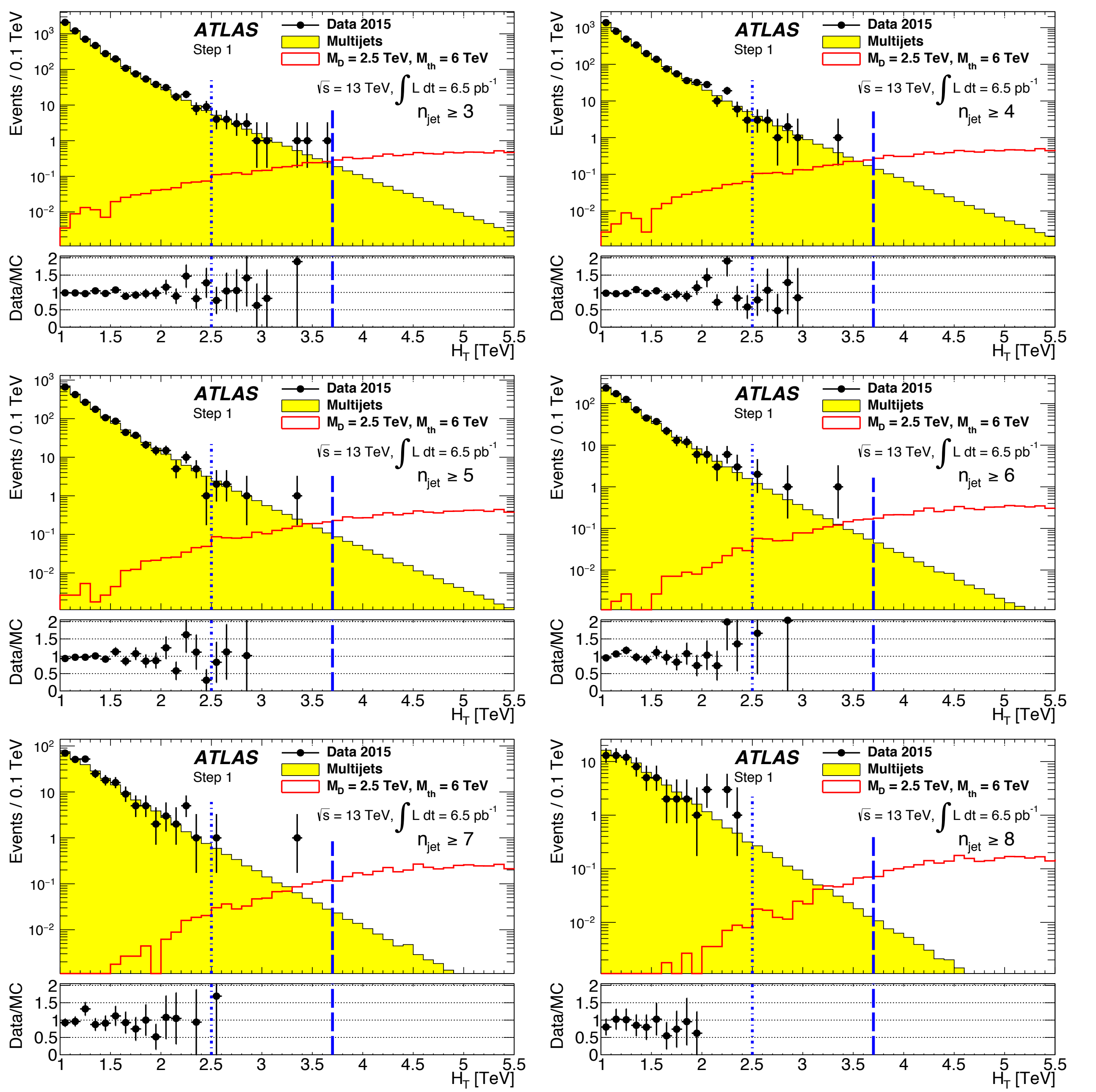

Figure 1: Data and MC simulation comparison for the distributions of the scalar sum of jet transverse momenta H_T in different inclusive n_{jet} bins for the 6.5 pb^{-1} data sample. The black hole signal with M_D = 2.5 TeV, M_{th} = 6.0 TeV is superimposed with the data and background MC simulation sample. The MC is normalized to data in the normalization region. The vertical dashed-dotted line marks the boundary between control region and validation region, and the dashed line marks the boundary between validation region and signal region. The boundaries shown correspond to those determined for the $n_{jet} \geq 3$ case.

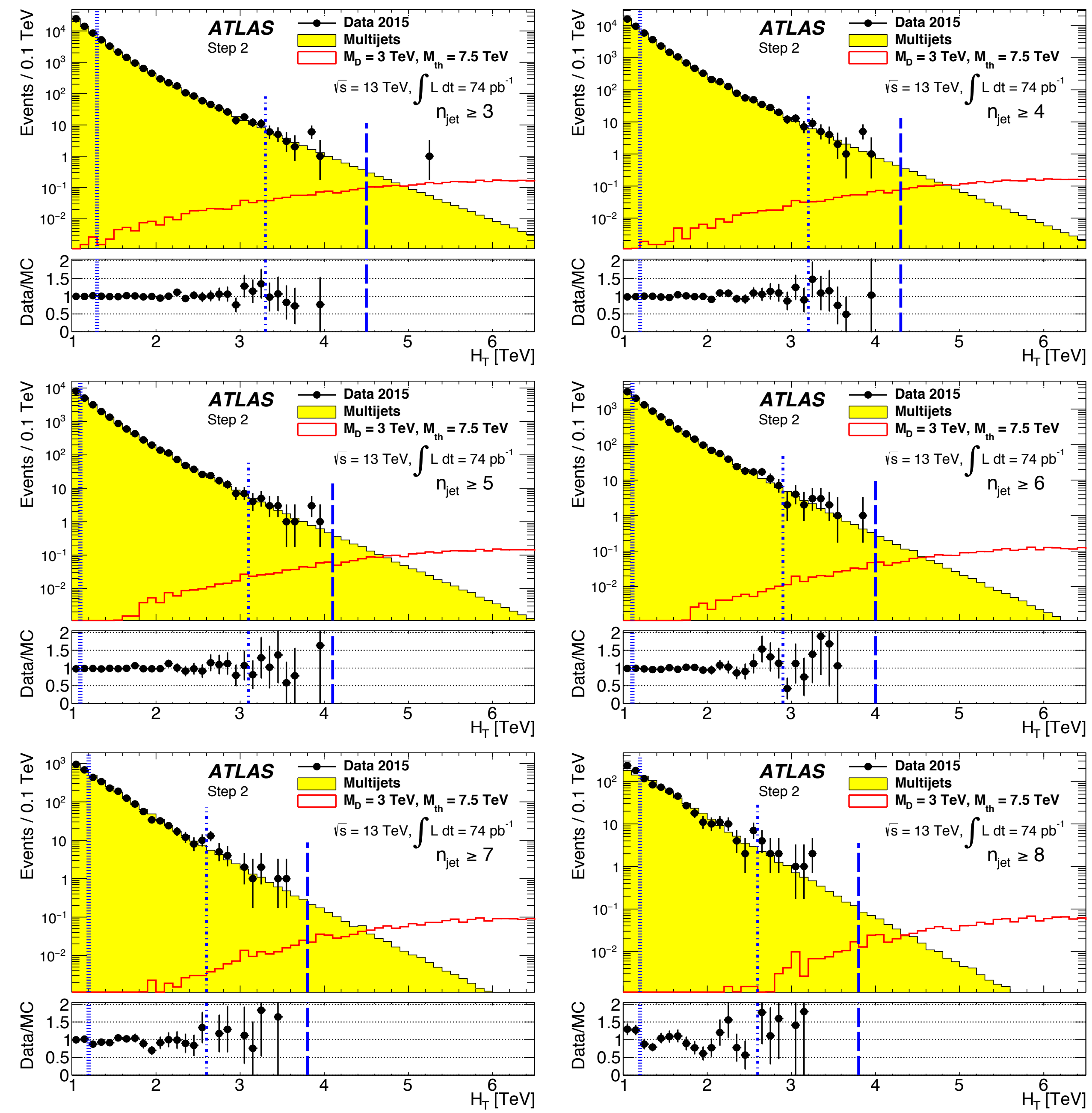

Figure 2: Data and MC simulation comparison for H_T distributions in different inclusive n_{jet} bins for the 74 pb^{-1} data sample. The black hole signal with M_D = 3 TeV, M_{th} = 7.5 TeV is superimposed with the data and background MC. The MC simulation was normalized to data in the normalization region. The vertical dotted line marks the lower boundary of the control region, the vertical dashed-dotted line marks the boundary between control region and validation region, and the vertical dashed line marks the boundary between validation region and signal region. These boundaries are determined for each n_{jet} sample separately.

ATLAS search for strong gravity in multi-jets

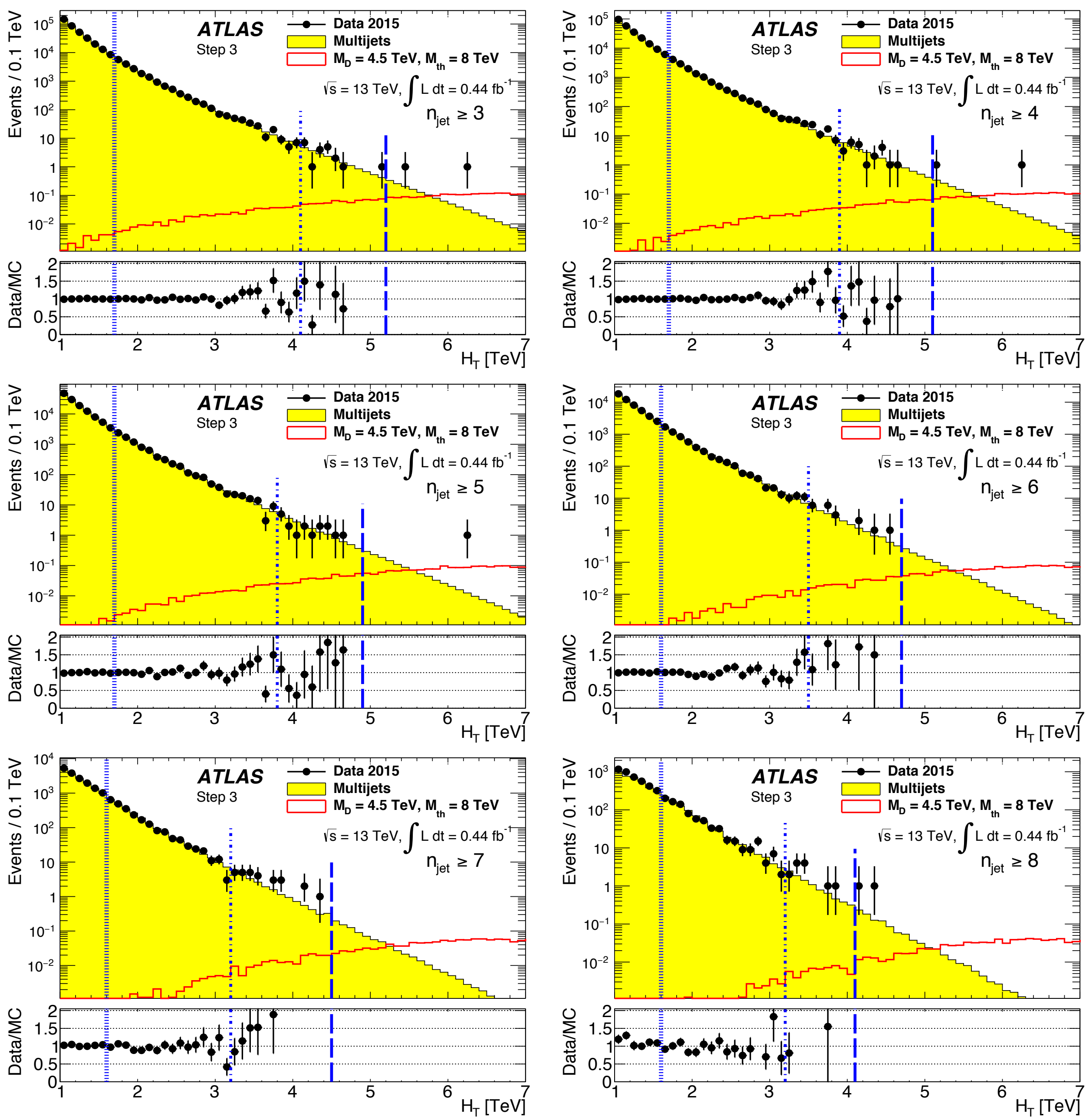

Figure 3: Data and MC simulation comparison for H_T distributions in different inclusive n_{jet} bins for the 0.44 fb^{-1} data sample. The black hole signal with M_D = 4.5 TeV, M_{th} = 8 TeV is superimposed with the data and background MC. The MC simulation is normalized to data in the normalization region. The vertical dotted line marks the lower boundary of the control region, the vertical dashed-dotted line marks the boundary between control region and validation region, and the vertical dashed line marks the boundary between validation region and signal region. These boundaries are determined for each n_{jet} sample separately.

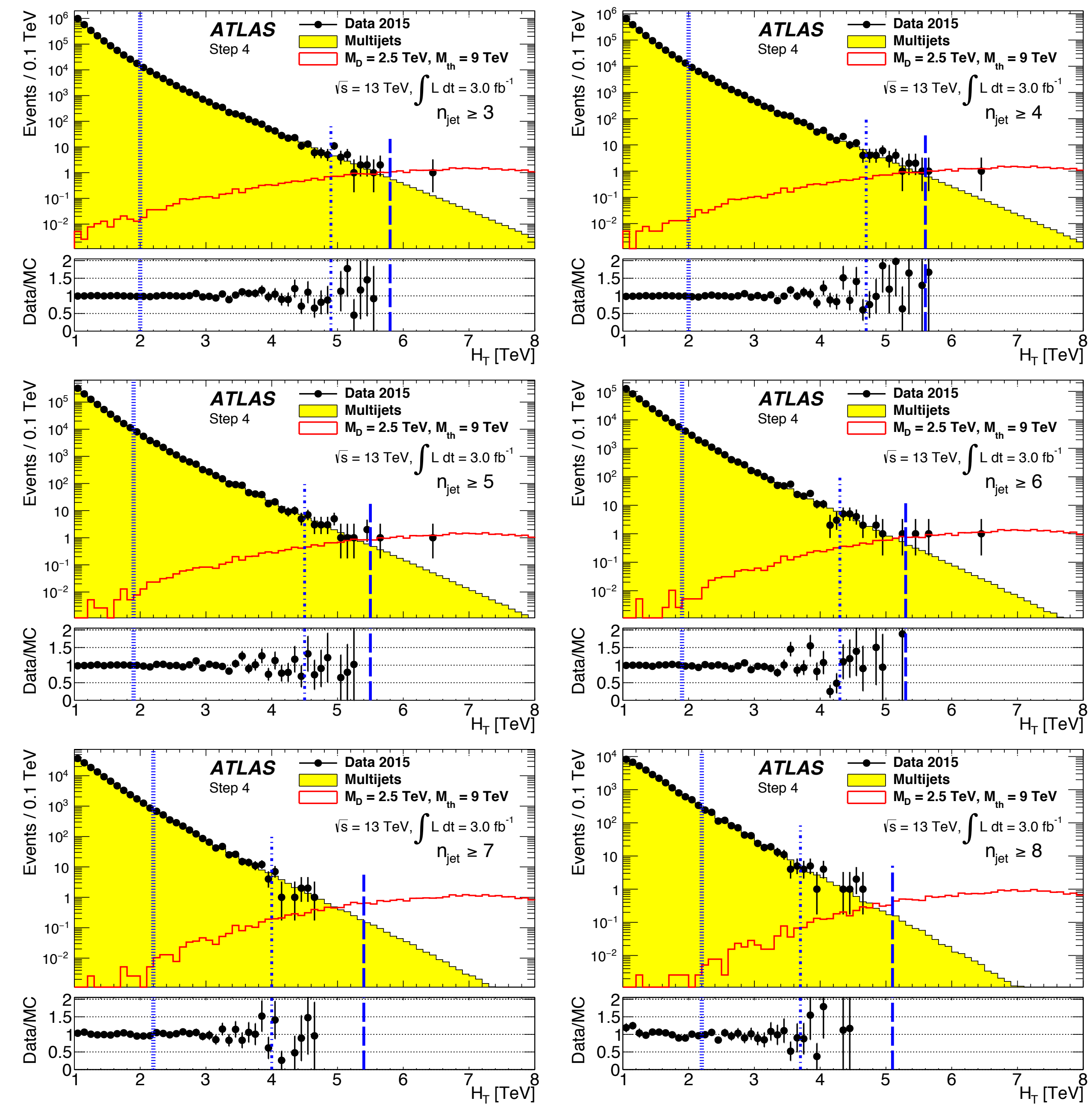

Figure 4: Data and MC simulation comparison for H_T distributions in different inclusive n_{jet} bins for the 3.0 fb^{-1} data sample. The black hole signal with M_D = 2.5 TeV, M_{th} = 9.0 TeV is superimposed with the data and background MC. The MC simulation is normalized to data in the normalization region. The vertical dotted line marks the lower boundary of the control region, the vertical dashed-dotted line marks the boundary between control region and validation region, and the vertical dashed line marks the boundary between validation region and signal region. These boundaries are determined for each n_{jet} sample separately.

ATLAS search for strong gravity in multi-jets

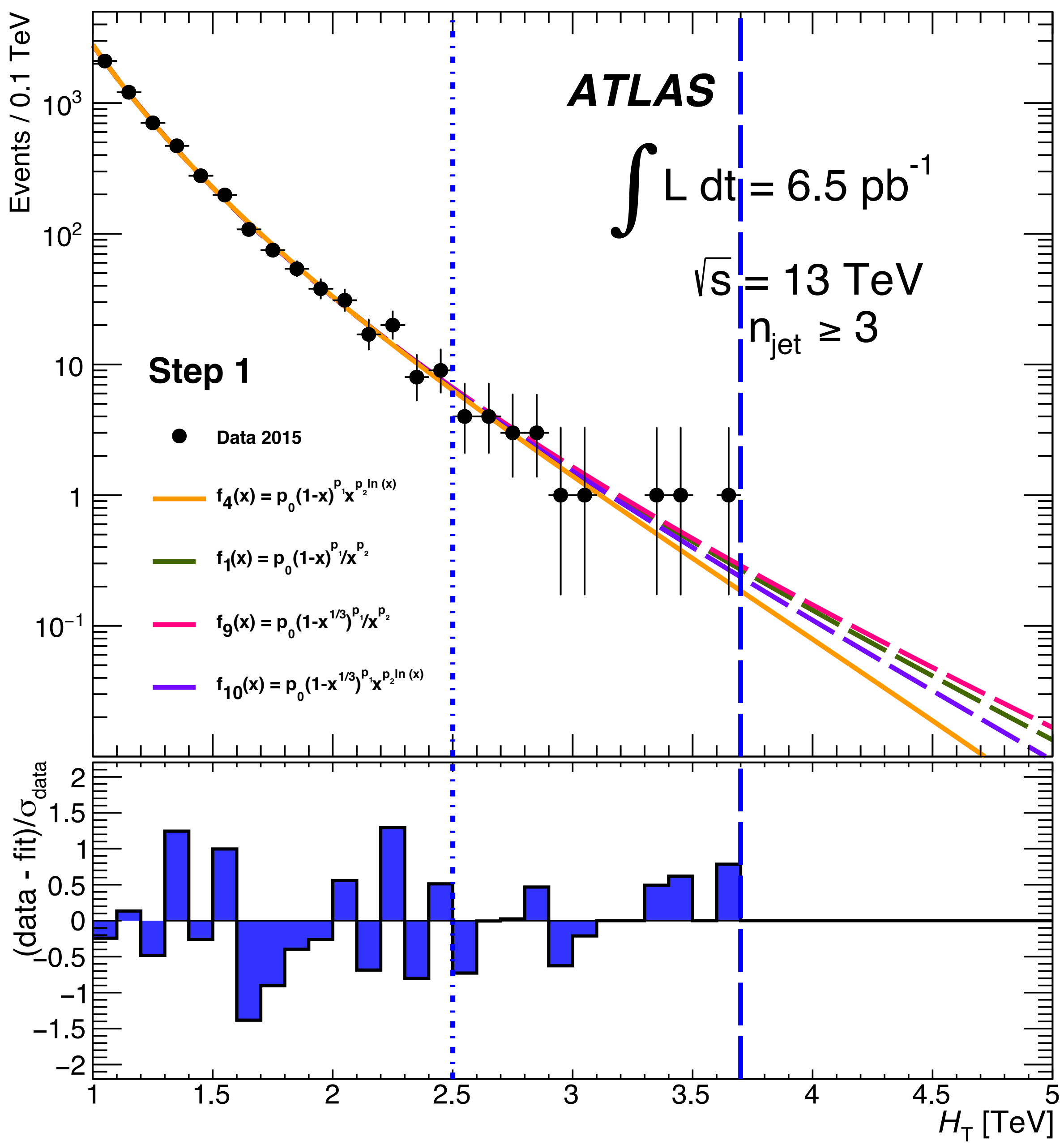

Figure 5: The data in 1.0 TeV < H_T < 2.5 TeV for $n_{jet} \geq 3$ are fitted by the baseline function (solid), and three alternative functions (dashed). The fitted functions are extrapolated to the validation region and signal region. The control, validation and signal regions are delimited by the vertical lines. The bottom section of the figure shows the residual significance defined as the ratio of the difference between fit and data over the statistical uncertainty of data, where the fit prediction is taken from the baseline function.

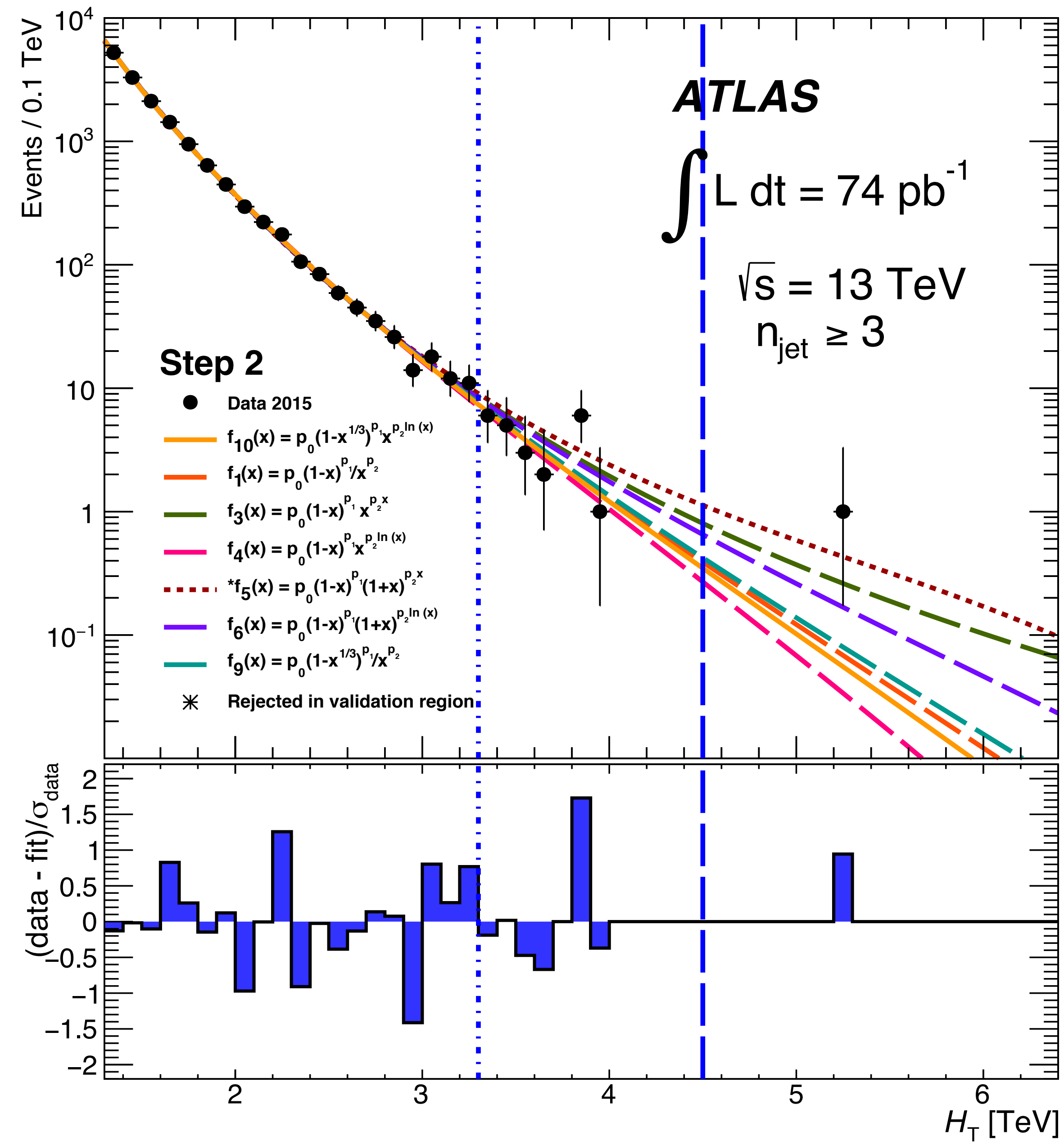

Figure 6: The data in 1.2 TeV < H_T < 3.3 TeV for $n_{jet} \geq 3$ are fitted by the baseline function (solid), and alternative functions (dashed). The fitted functions are extrapolated to the validation and signal region. control, validation and signal regions are delimited by the vertical lines. The function indicated by an aste is rejected at 95% CL by the data in the validation region. The bottom section of the figure shows the resi significance defined as the ratio of the difference between fit and data over the statistical uncertainty of data, w the fit prediction is taken from the baseline function.

ATLAS search for strong gravity in multi-jets

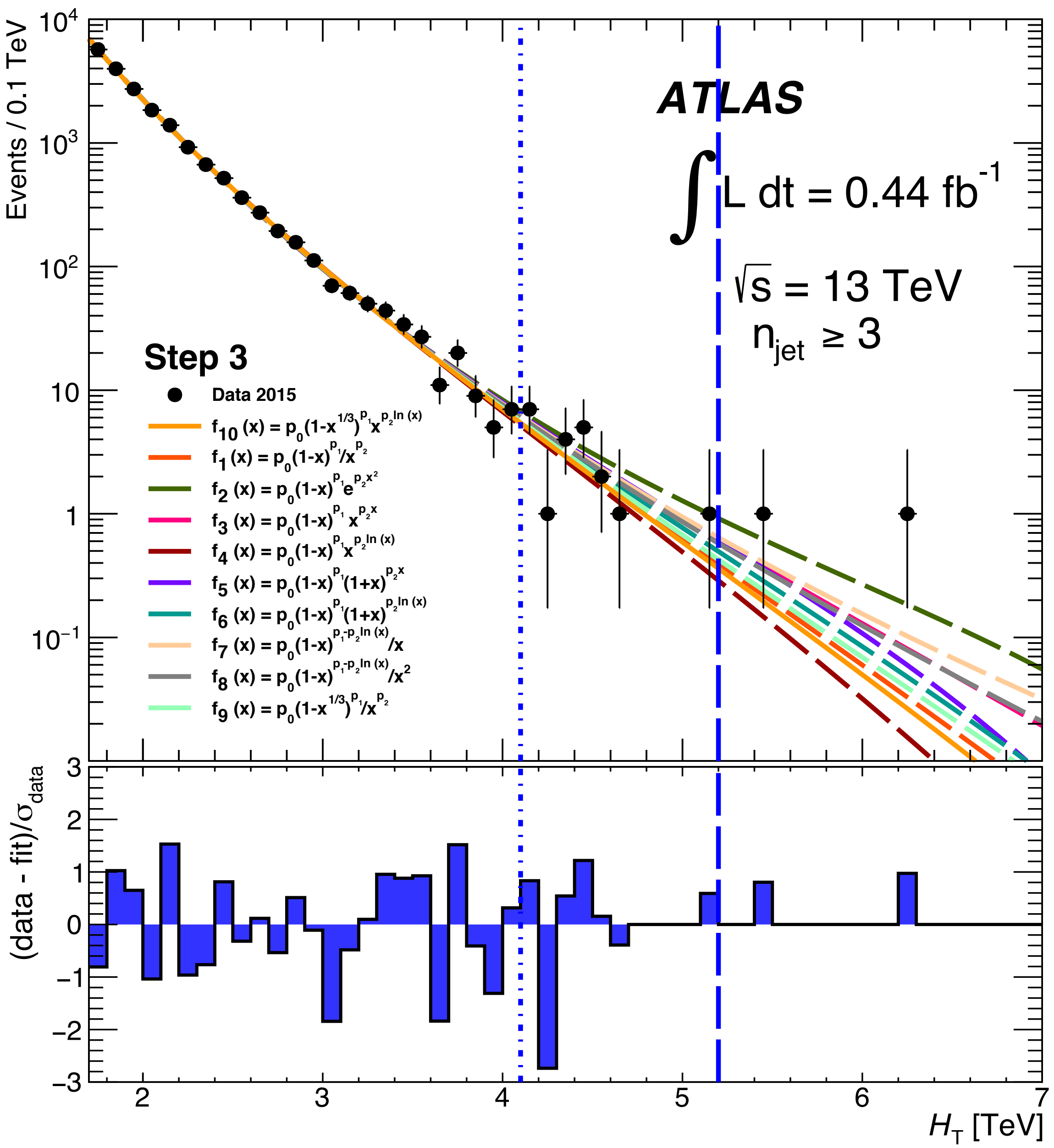

Figure 7: The data in 1.7 TeV < H_T < 4.1 TeV for $n_{jet} \geq 3$ are fitted by the baseline function (solid), and nine alternative functions (dashed). The fitted functions are extrapolated to the validation region and signal region. The control, validation and signal regions are delimited by the vertical lines. The bottom section of the figure shows the residual significance defined as the ratio of the difference between fit and data over the statistical uncertainty of data, where the fit prediction is taken from the baseline function.

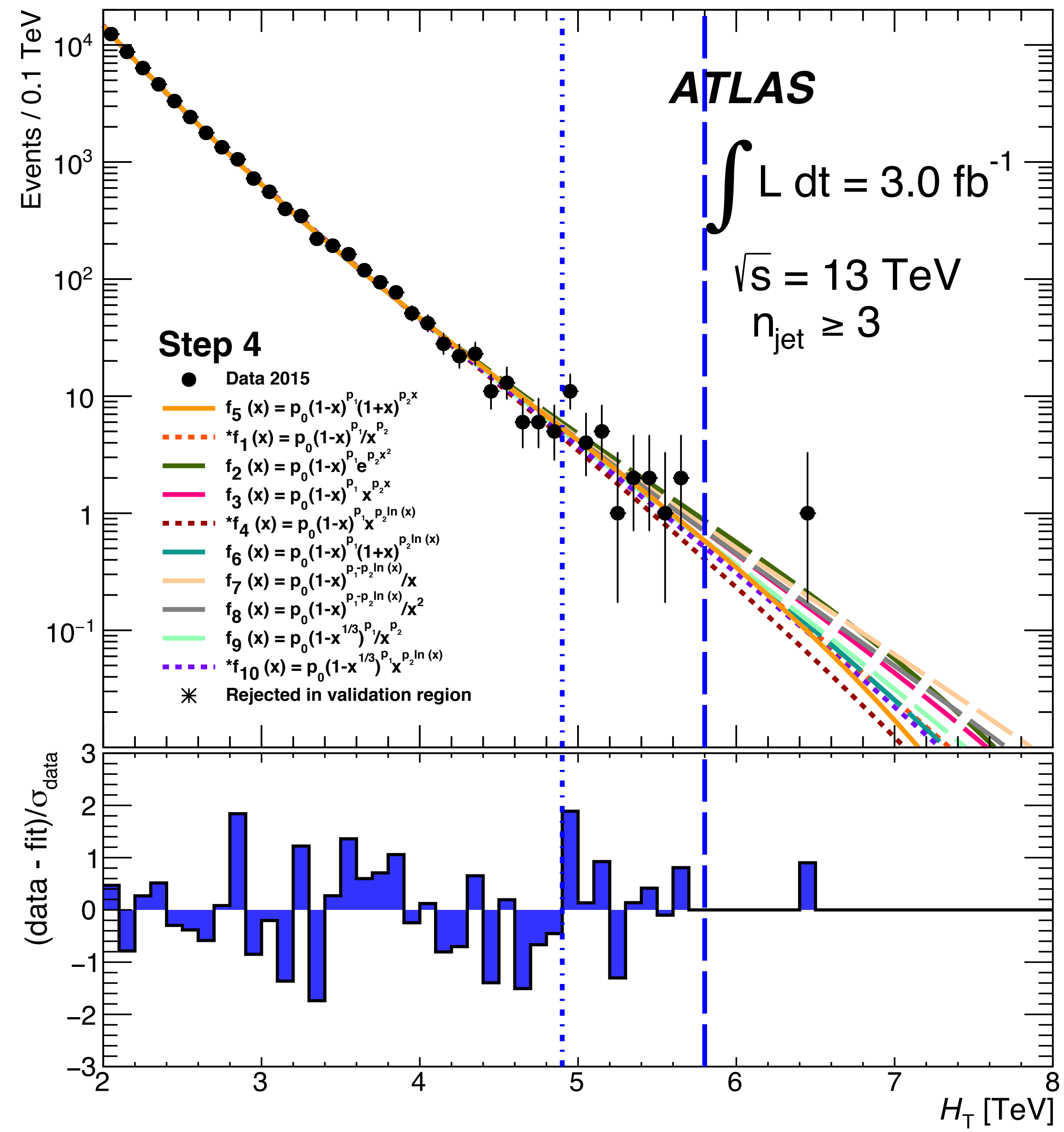

Figure 8: The data in 2.0 TeV < H_T < 4.9 TeV for $n_{jet} \geq 3$ are fitted by the baseline function (solid), and nine alternative functions (dashed). The fitted functions are extrapolated to the validation region and signal region. The control, validation and signal regions are delimited by the vertical lines. The three functions indicated by asterisks are rejected at 95% CL by the data in the validation region. The bottom section of the figure shows the residual significance defined as the ratio of the difference between fit and data over the statistical uncertainty of data, where the fit prediction is taken from the baseline function.

ATLAS search for strong gravity in multi-jets

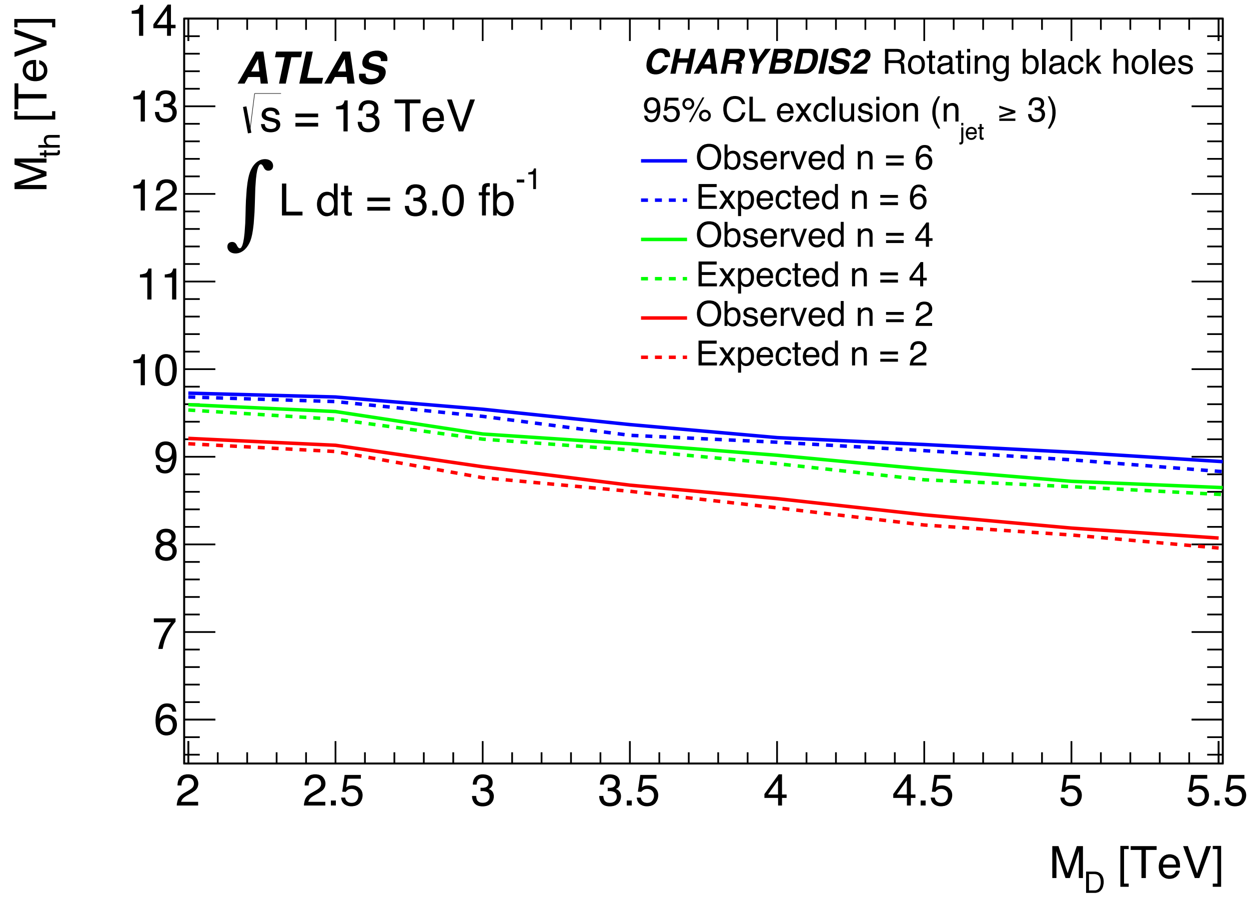

Figure 9: The observed and expected 95% CL exclusion limits on rotating black holes with different numbers of extra dimensions ($n = 2, 4, 6$) in the $M_{\mathrm{D}} - M_{\mathrm{th}}$ grid.. The results are based on the analysis of 3.0 fb^{-1} of integrated luminosity. The region below the lines is excluded.

$n_{\mathrm{jet}} \geq$	$H_{\mathrm{T}} > H_{\mathrm{T}}^{\mathrm{min}}$ (TeV)	Expected limit (fb)	Observed limit (fb)
3	5.8	$1.63^{+0.70}_{-0.57}$	1.33
4	5.6	$1.77^{+0.70}_{-0.57}$	1.77
5	5.5	$1.56^{+0.73}_{-0.50}$	1.75
6	5.3	$1.52^{+0.69}_{-0.50}$	2.15
7	5.4	$1.02^{+0.36}_{-0.0}$	1.02
8	5.1	$1.01^{+0.29}_{-0.0}$	1.01

Table 6: The expected and observed limits on the inclusive cross section in femtobarns for production of events as a function of n_{jet} and the minimum value of H_{T} . The limits are derived from results of the 3.0 fb^{-1} analysis so $H_{\mathrm{T}}^{\mathrm{min}}$ corresponds to the value of S for the last analysis step.

ATLAS search for strong gravity in multi-jets

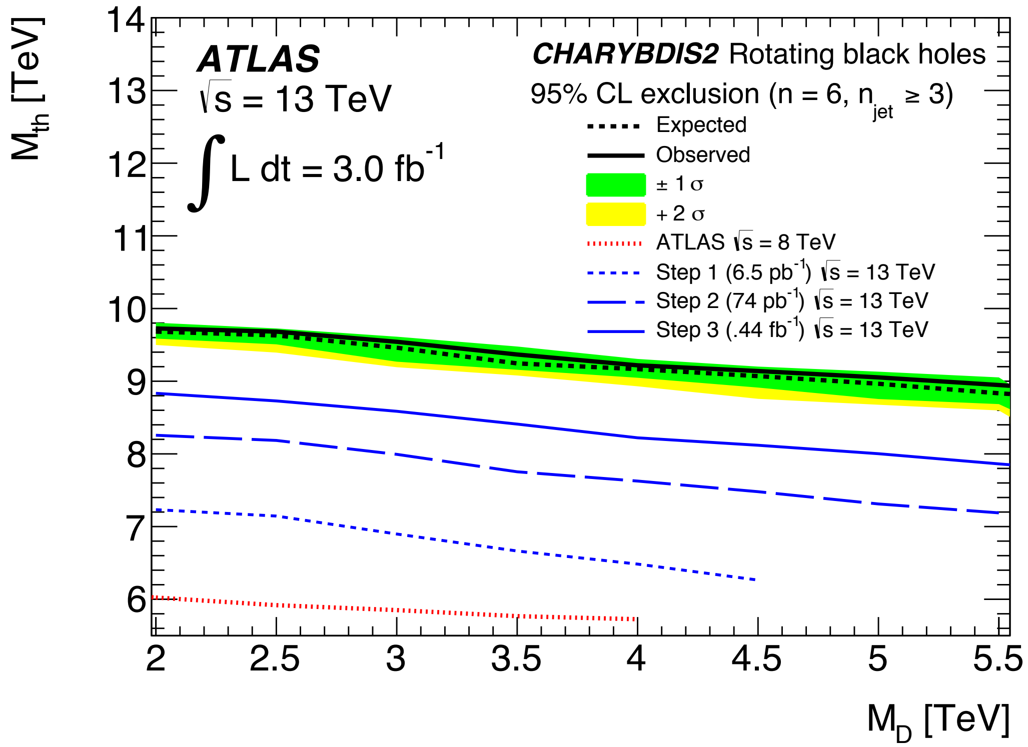

Figure 10: "The observed and expected limits on rotating black holes with $n = 6$ in the $M_D - M_{th}$ grid, from the analysis with an integrated luminosity of 3.0 fb^{-1}. The 95% CL expected limit is shown as the black dashed line, and limits corresponding to the $\pm 1\,\sigma$ and $+ 2\,\sigma$ variations of the background expectation are shown as the green and yellow bands, respectively. The 95% CL observed limit is shown as the black solid line. The $-2\,\sigma$ band is not shown as it almost completely overlaps with the $-1\,\sigma$ band. The blue dashed lines corresponds to the observed limits from the first, second and thirdstep analyses. The red dotted line corresponds to the limit from Run-1 ATLAS multijet search [5].

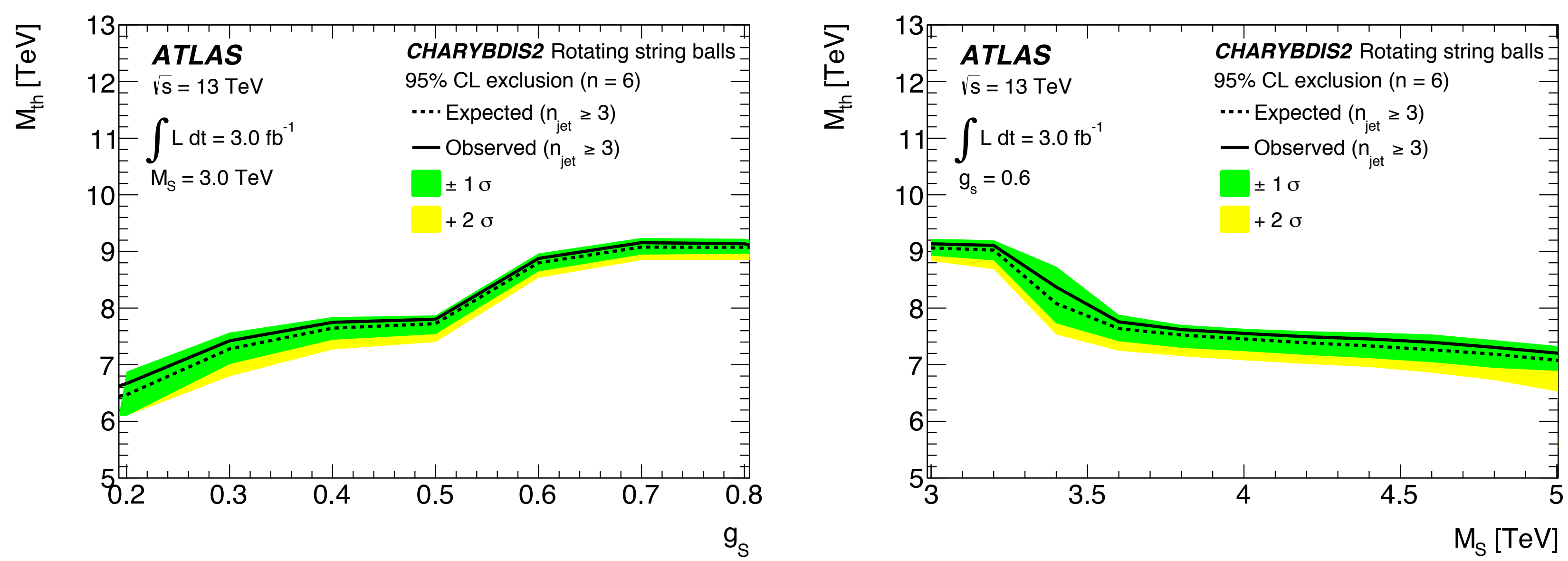

Figure 11: The expected and observed limits on the string ball model with $n = 6$, from the analysis with an integrated luminosity of 3.0 fb^{-1}. The left plot shows the 95% CL limit as a function of g_S and M_{th} (solid line). The dashed line shows the expected limit; the limits corresponding to the $\pm 1\,\sigma$ and $+ 2\,\sigma$ variations of the background The $-2\,\sigma$ band is not shown as it almost completely overlaps with the $-1\,\sigma$ band. expectation are shown as the green and yellow bands, respectively. The right plot shows the limits as a function of M_{th} and M_S for $g_S = 0.6$.

ATLAS di-b-jet resonance search

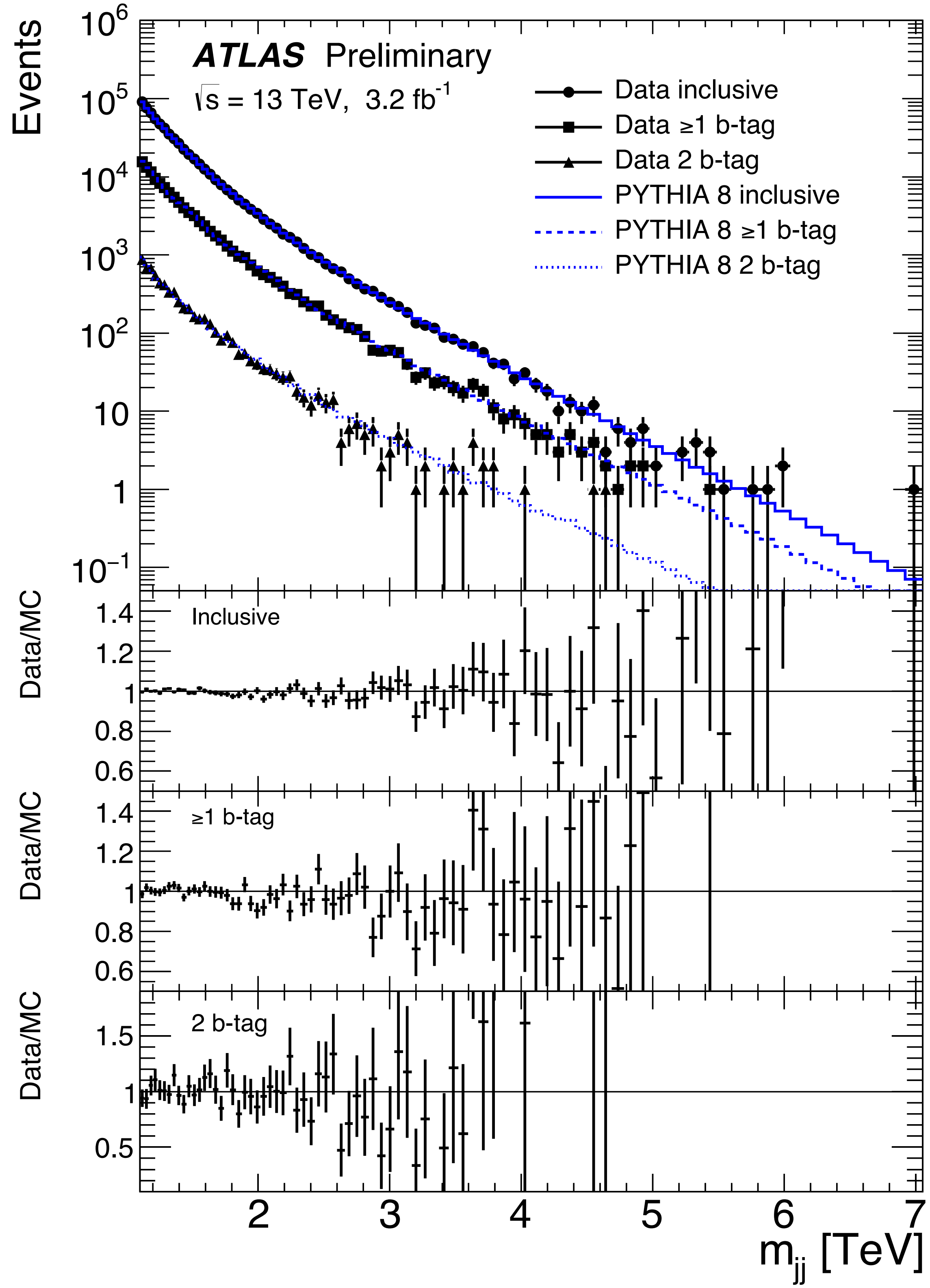

ATLAS di-b-jet resonance search

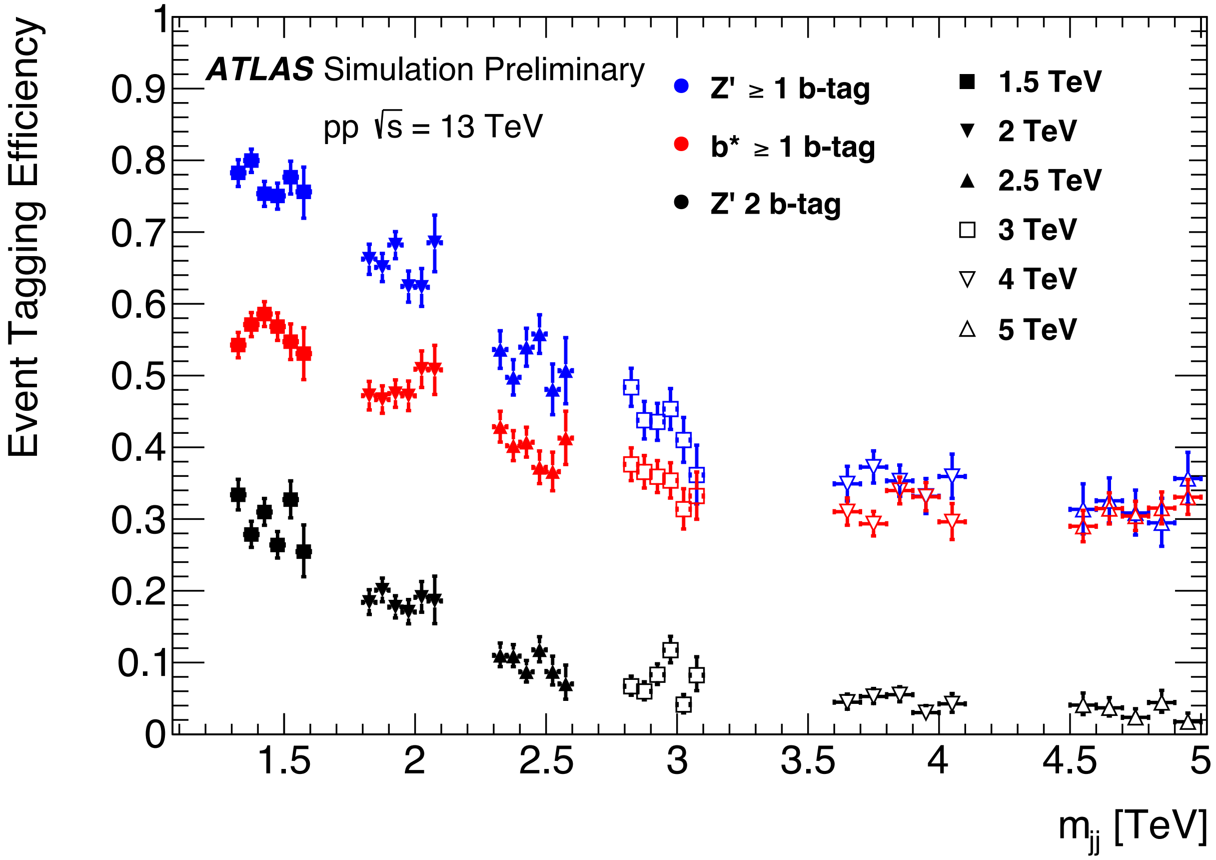

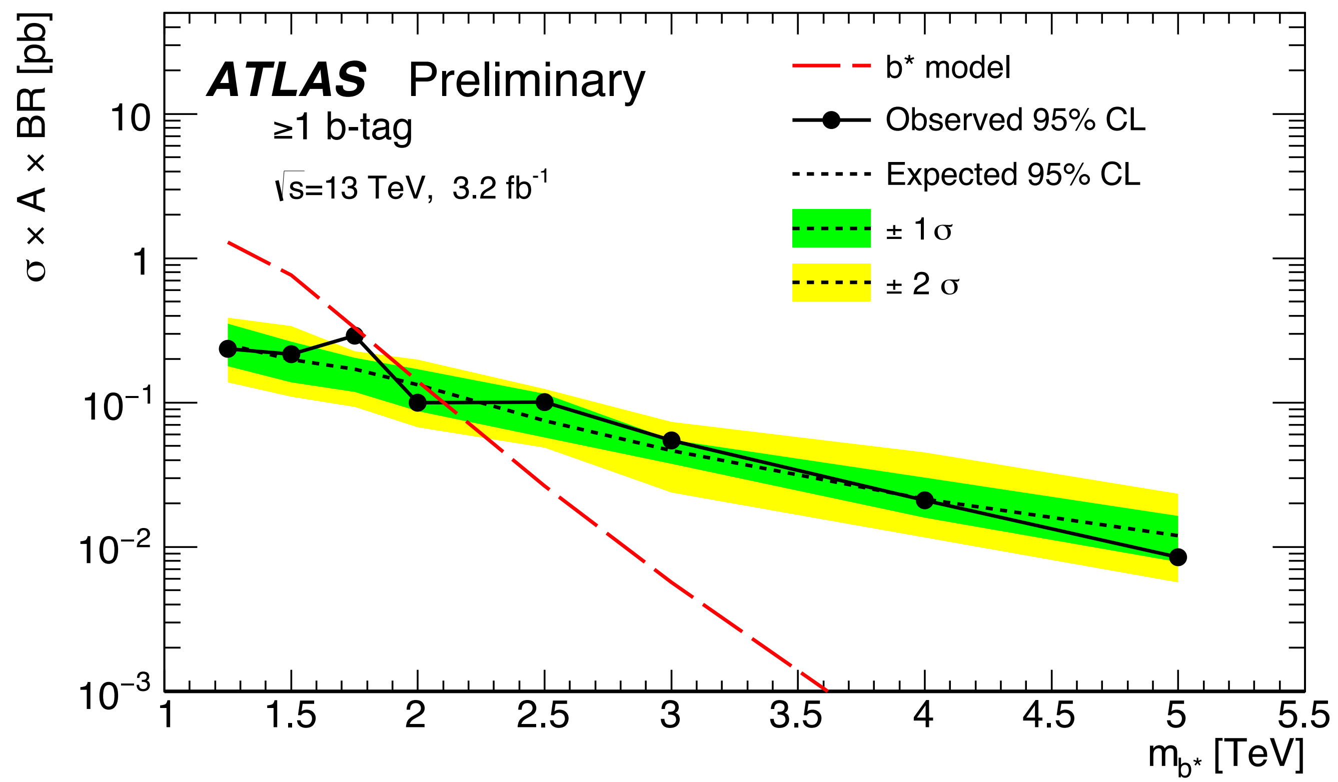

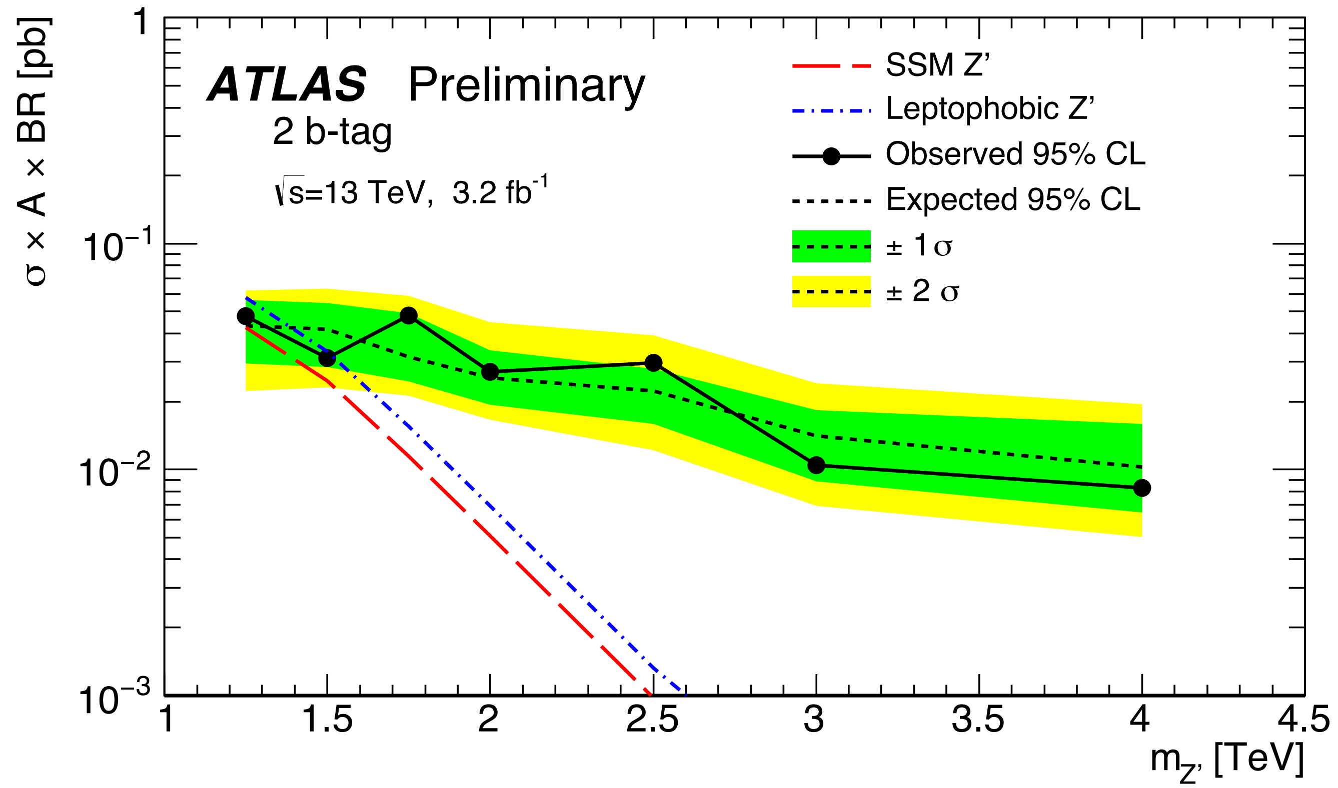

ATLAS di-b-jet resonance search

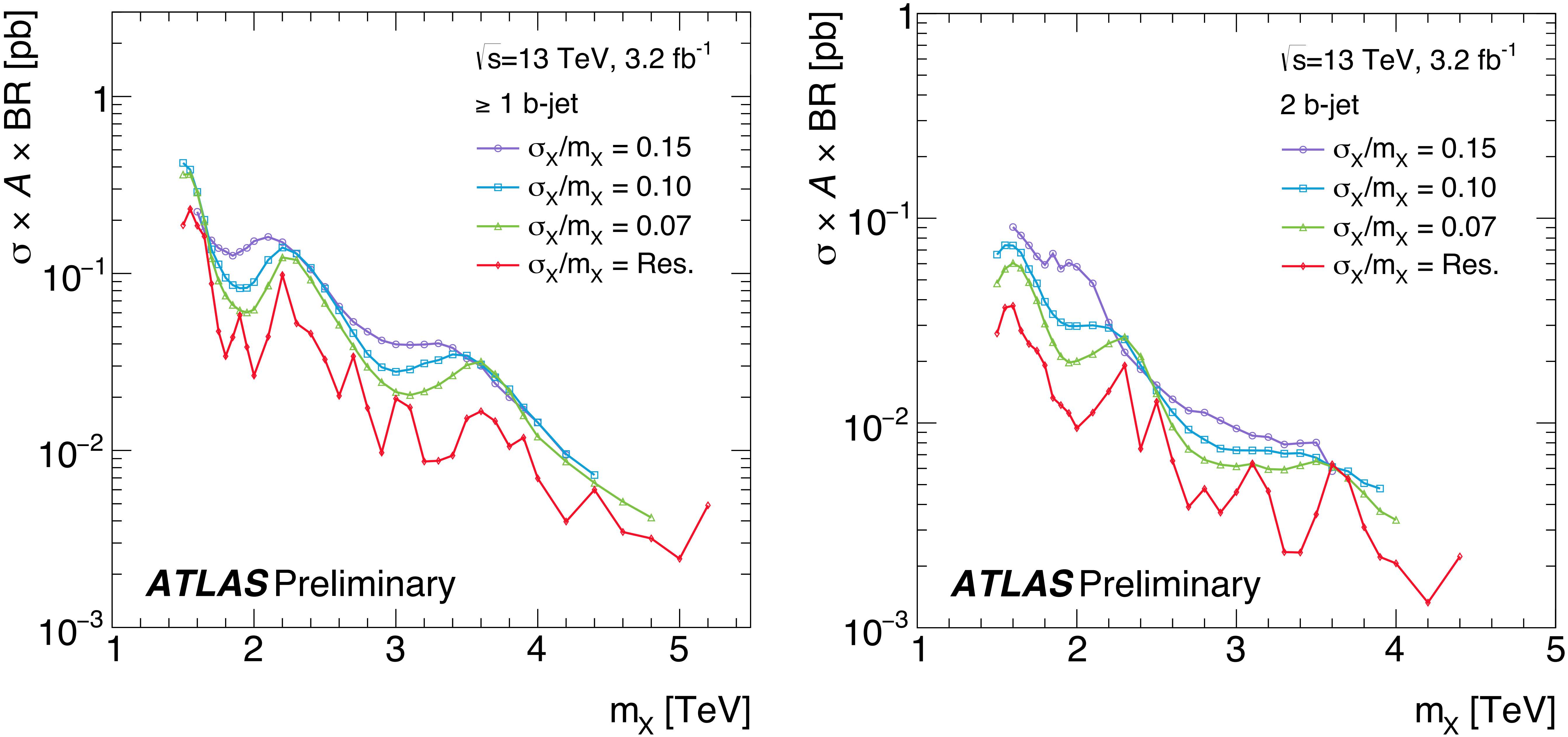

ATLAS di-b-jet resonance search

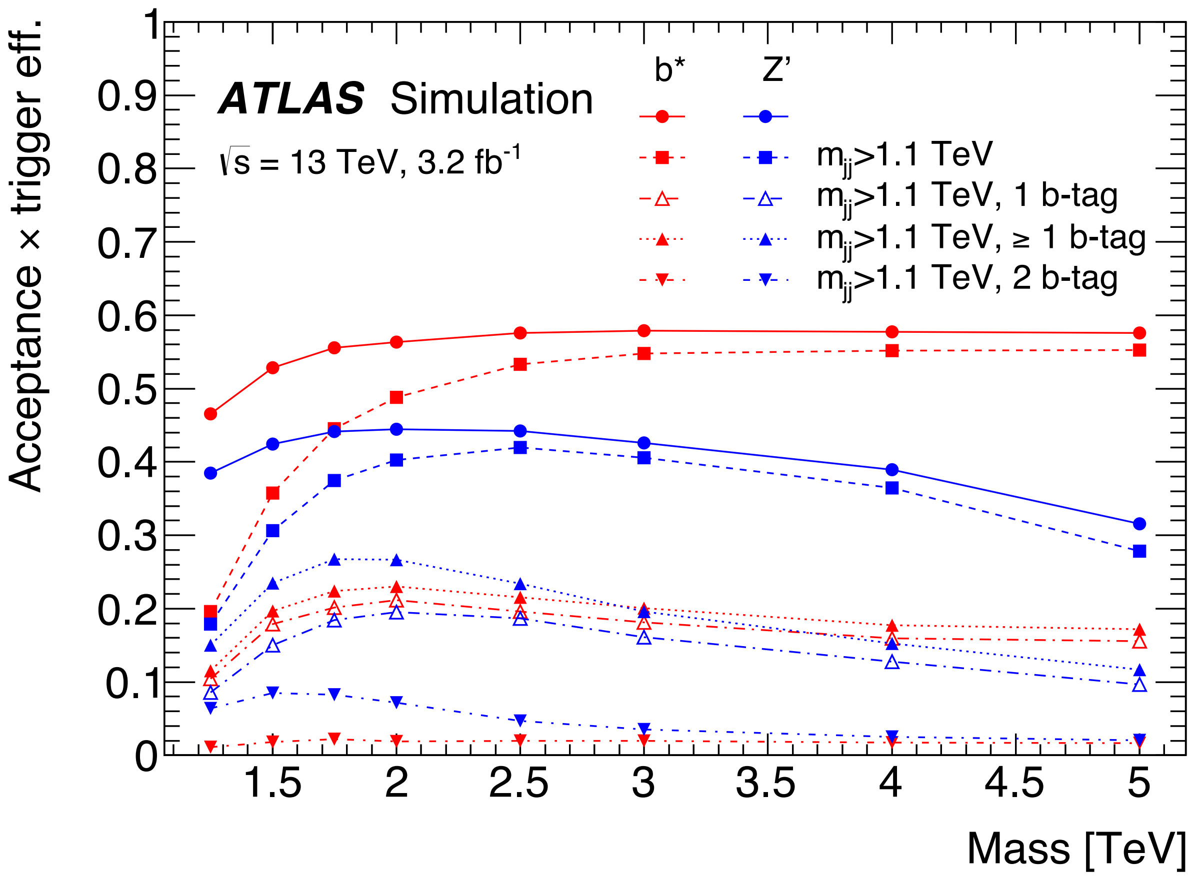

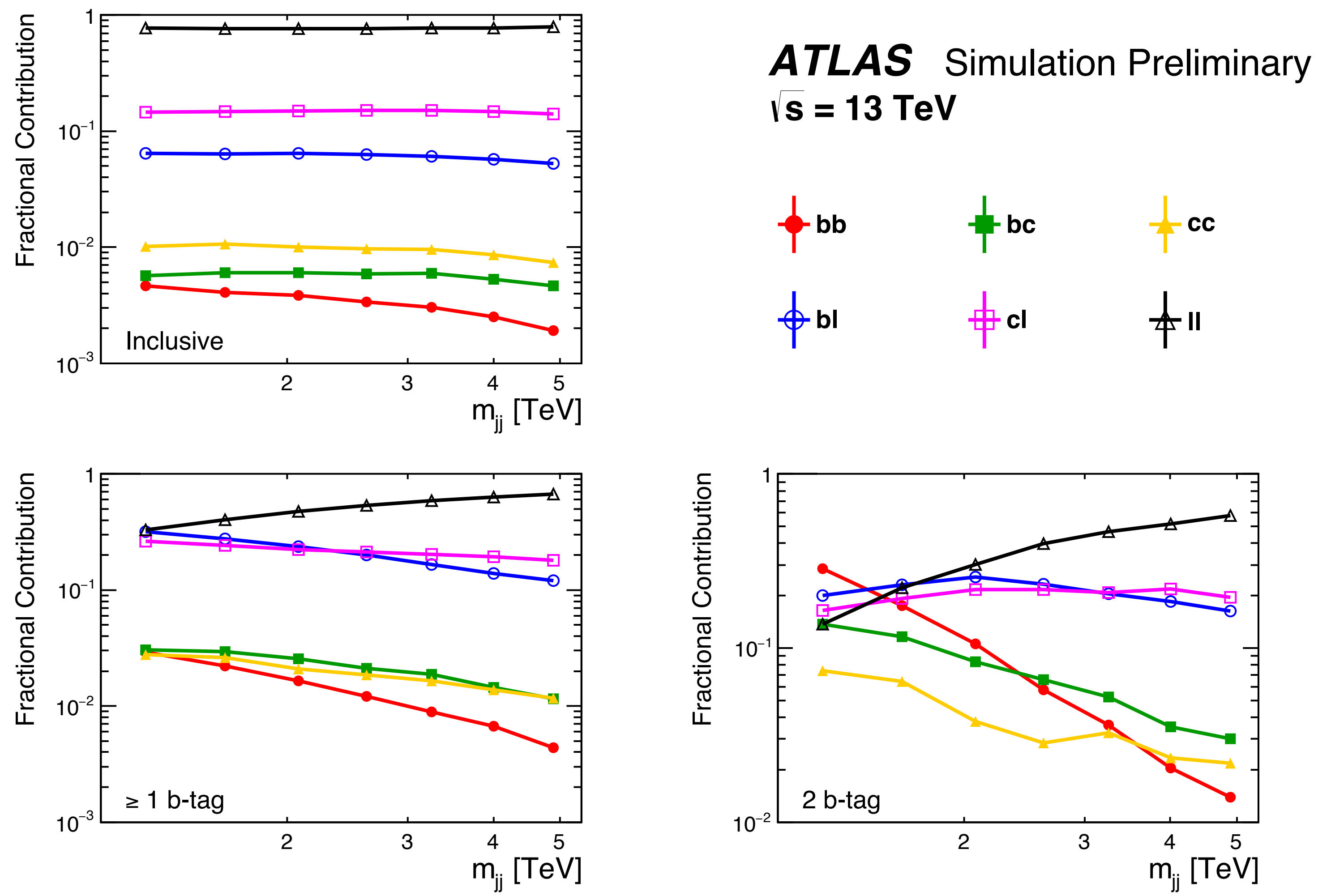

CMS leptoquark pair search in μμjj

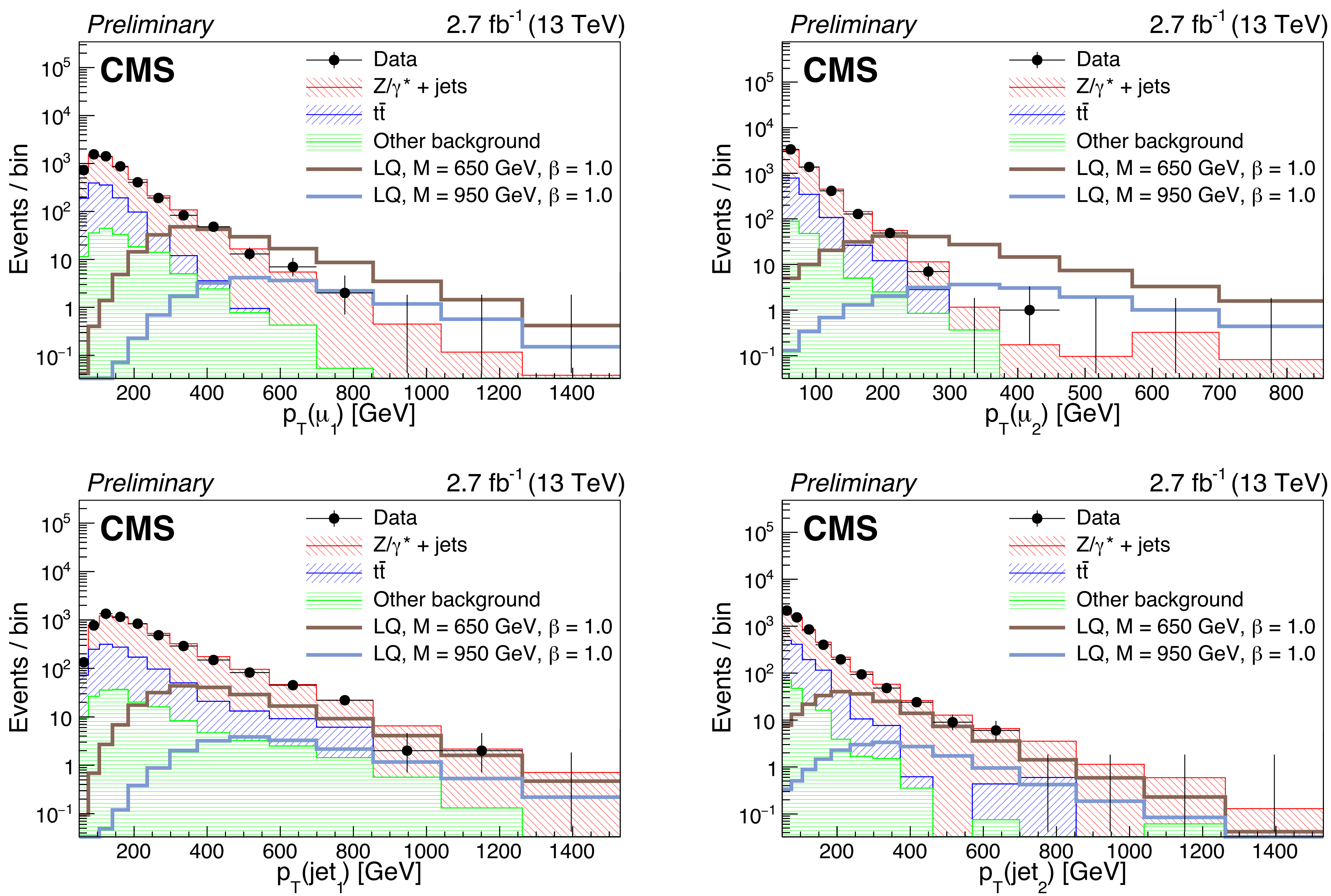

Figure 1: Distributions of the muon and the jet p_T's at preselection level. The contribution denoted as "Other Background" includes diboson, W+jets, and single-top contributions. Signal distributions are overlaid for LQ masses of 650 and 950 GeV.

CMS leptoquark pair search in μμjj

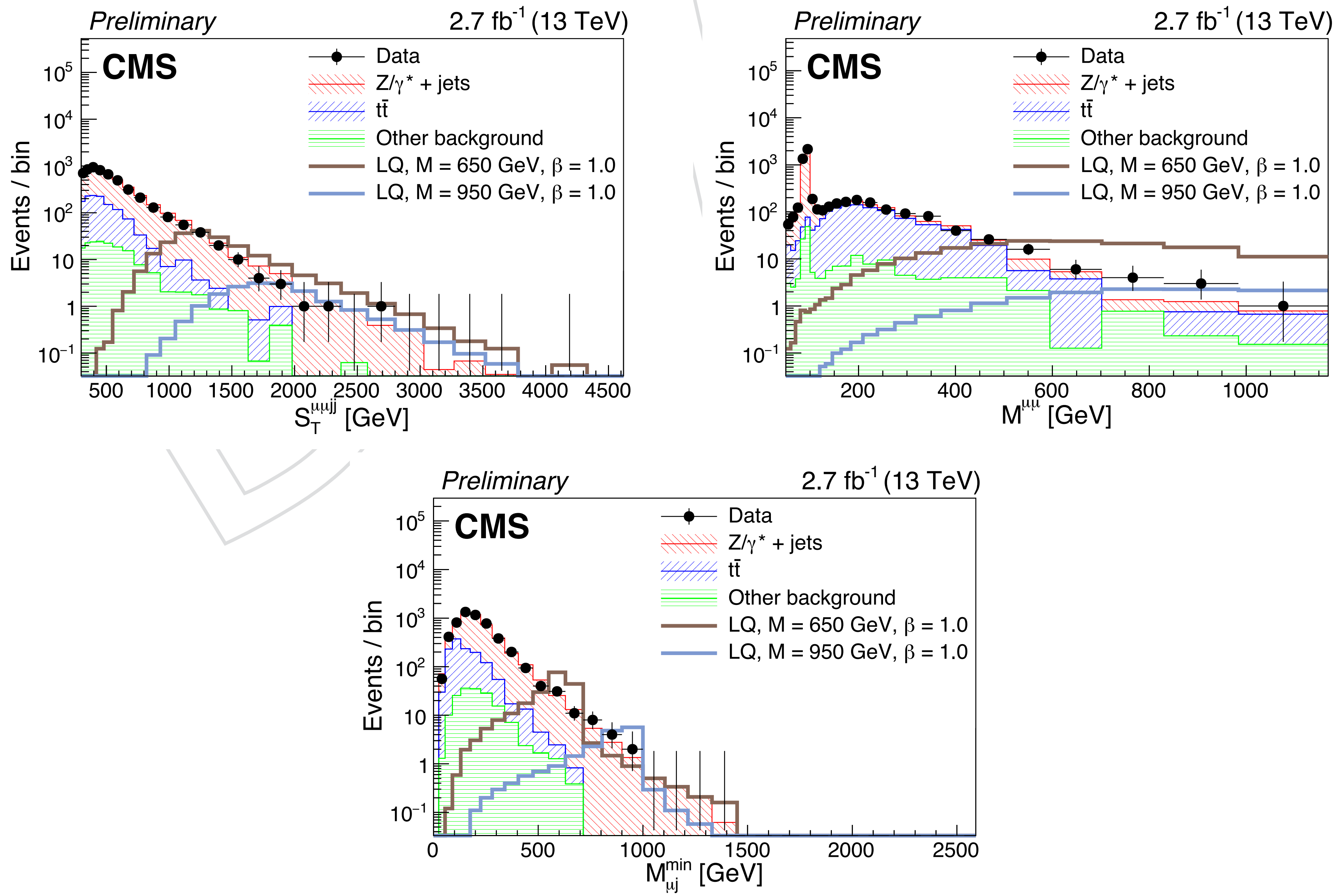

Figure 2: Distributions of S_T, $M_{\mu\mu}$, and of $M_{min}(\mu, \text{jet})$ at preselection level. The contribution denoted as "Other Background" includes diboson, W+jets, and single-top contributions. Signal distributions are overlaid for LQ masses of 650 and 950 GeV.

CMS leptoquark pair search in μμjj

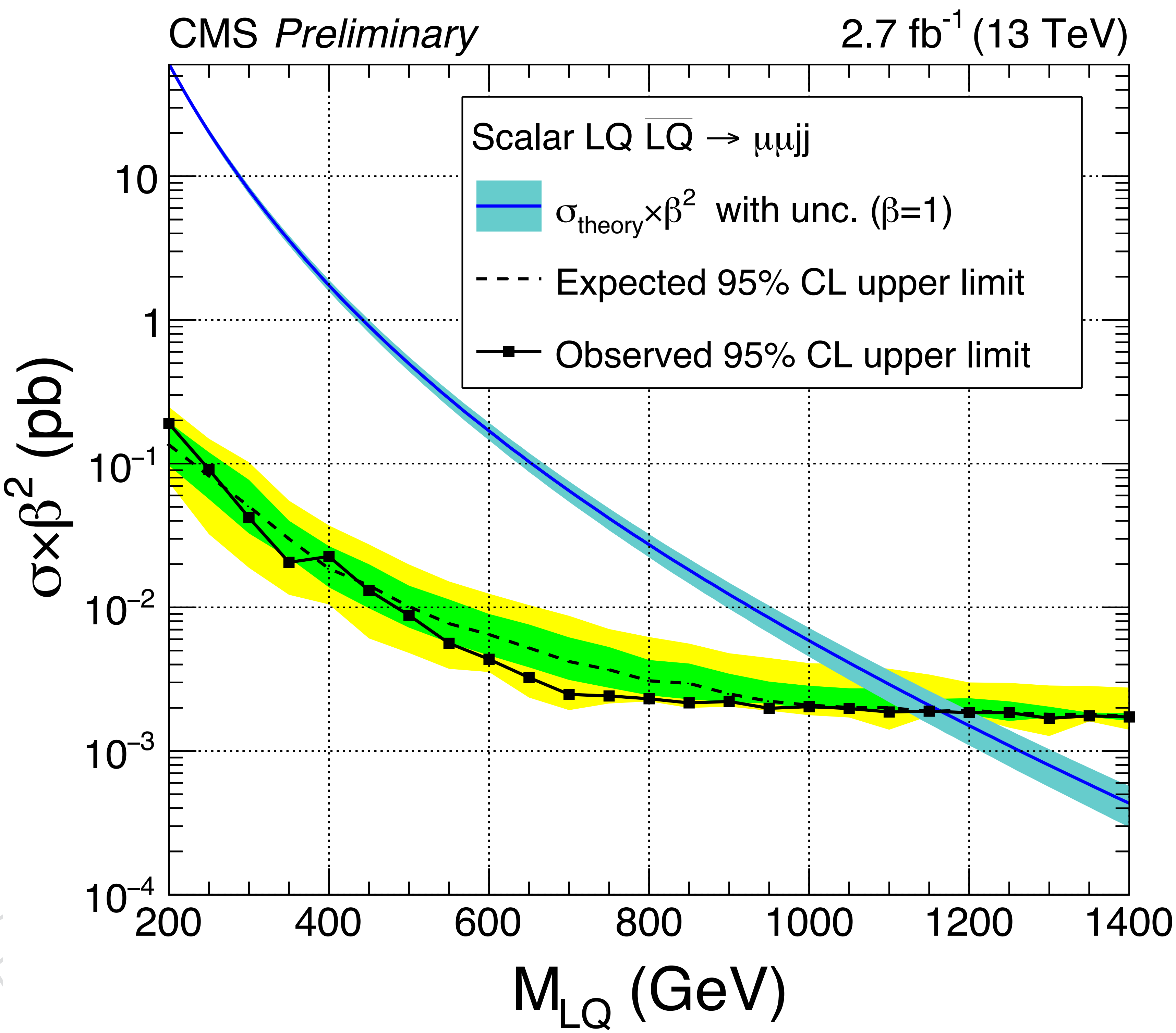

ATLAS search for strong gravity in l+jets

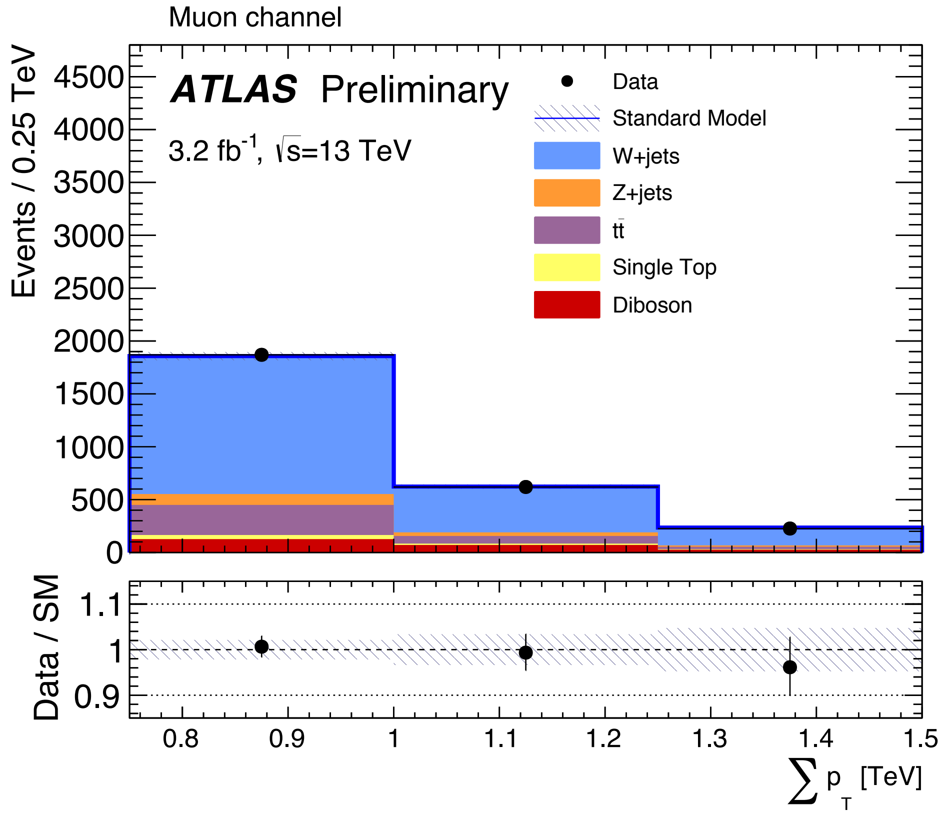

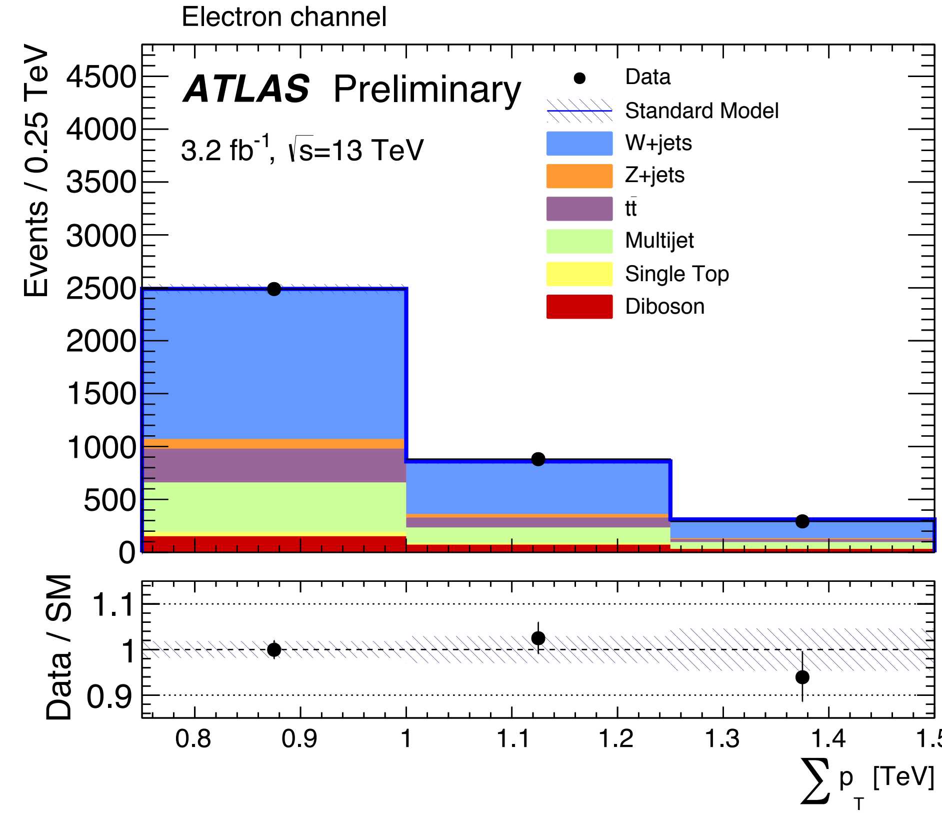

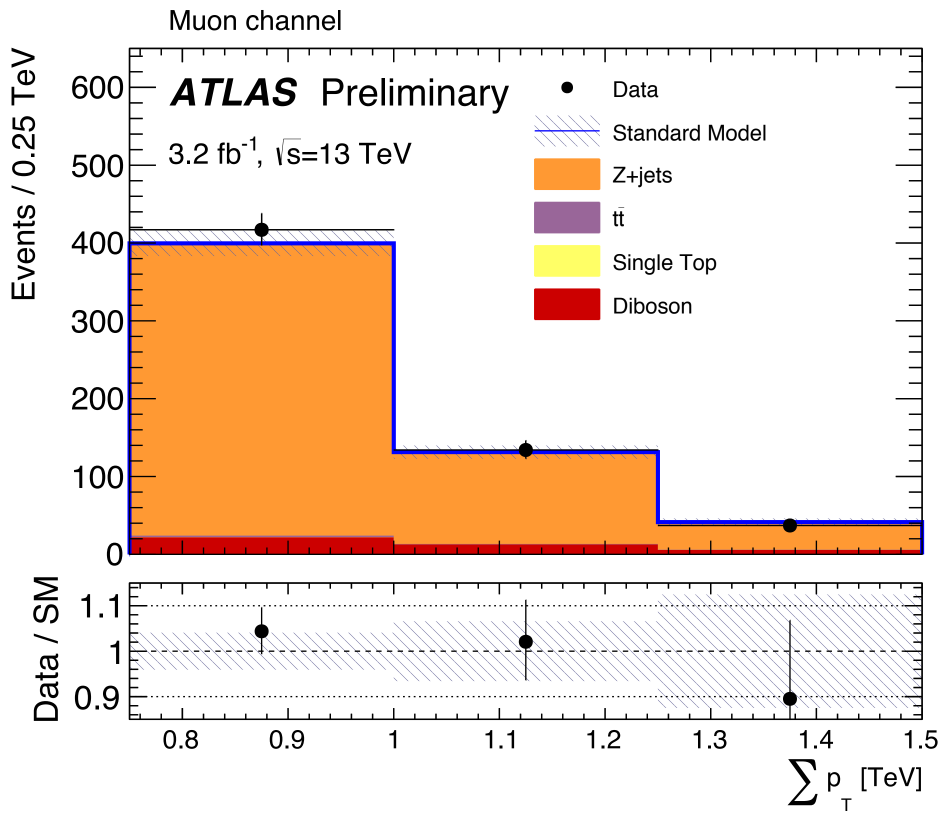

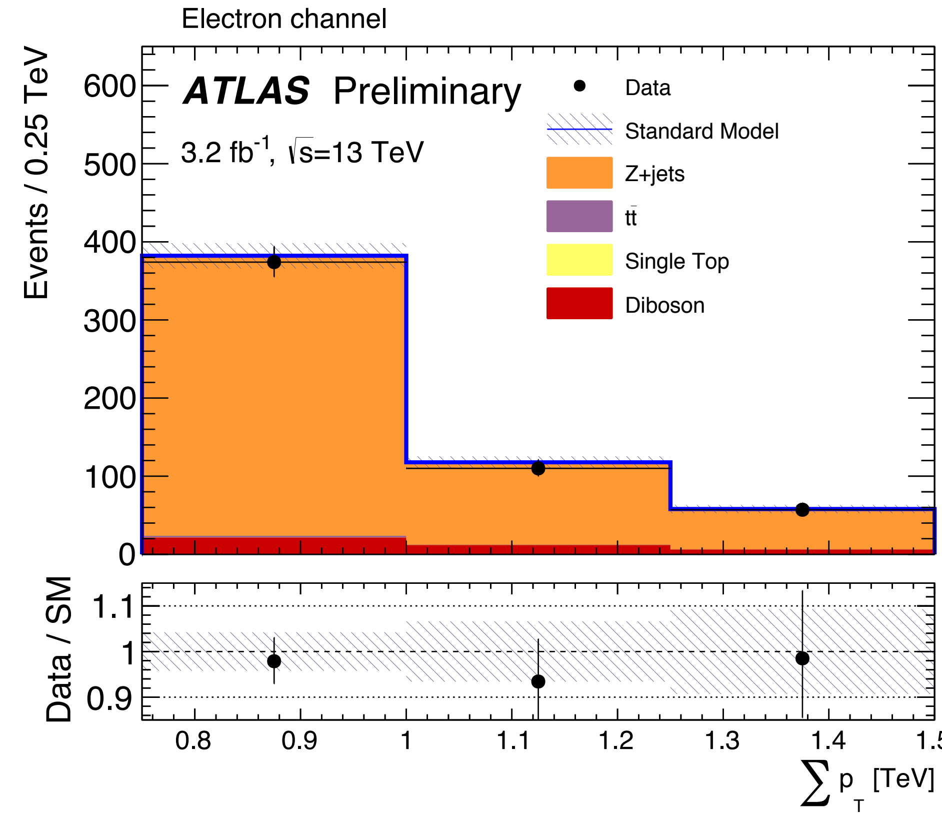

ATLAS search for strong gravity in l+jets

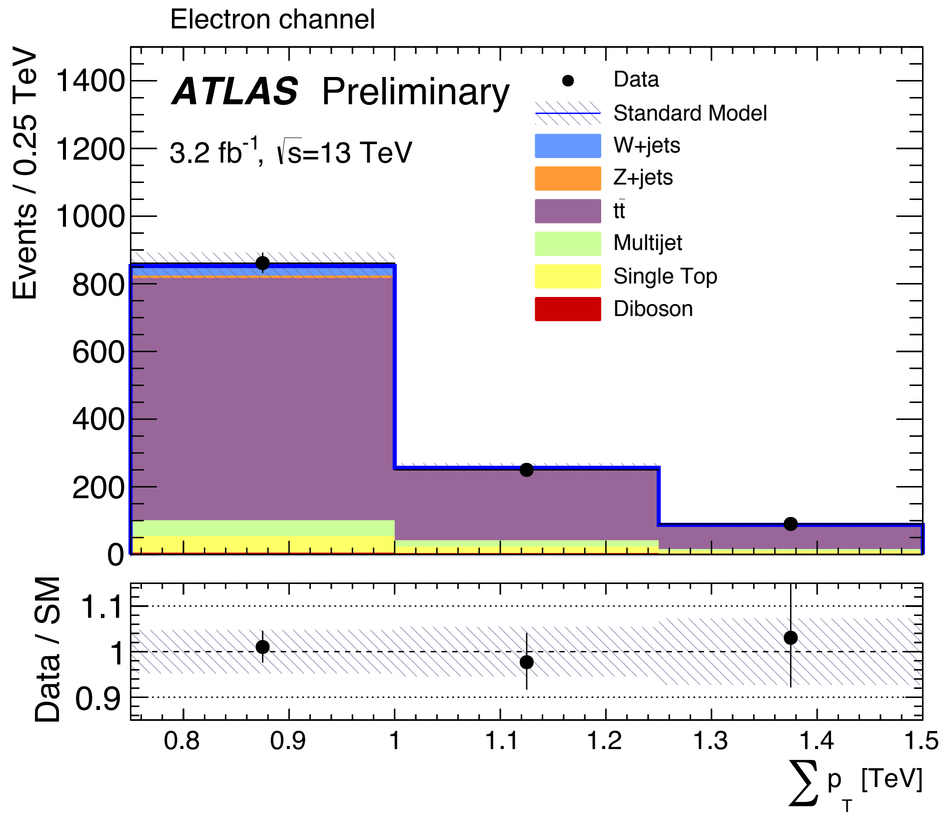

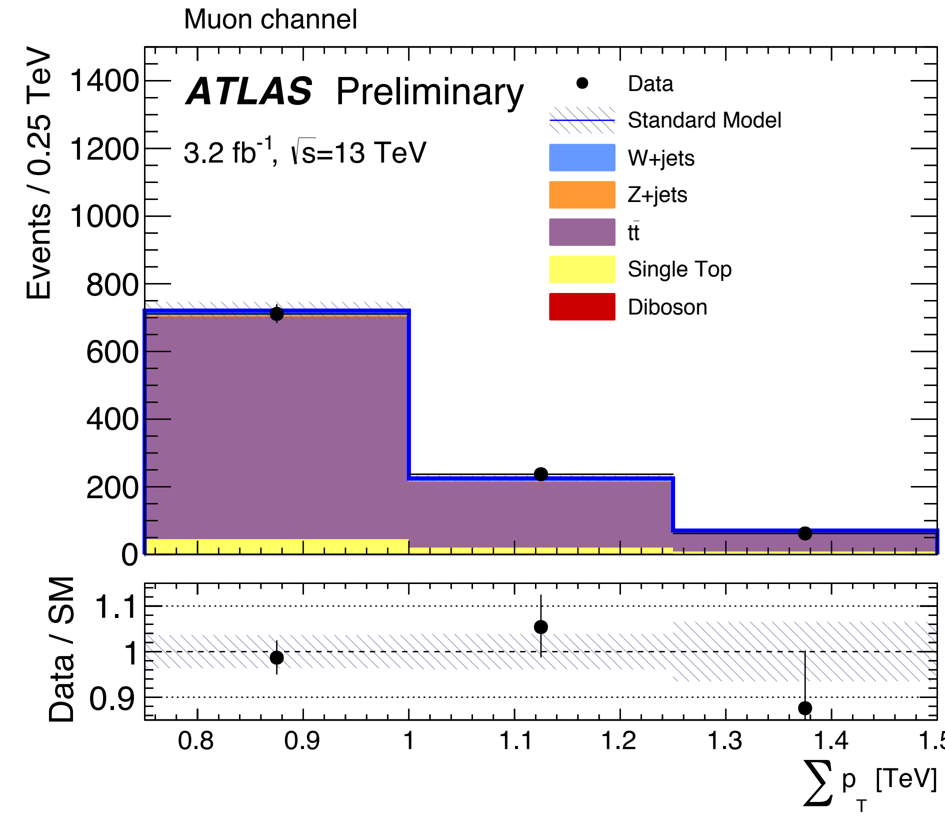

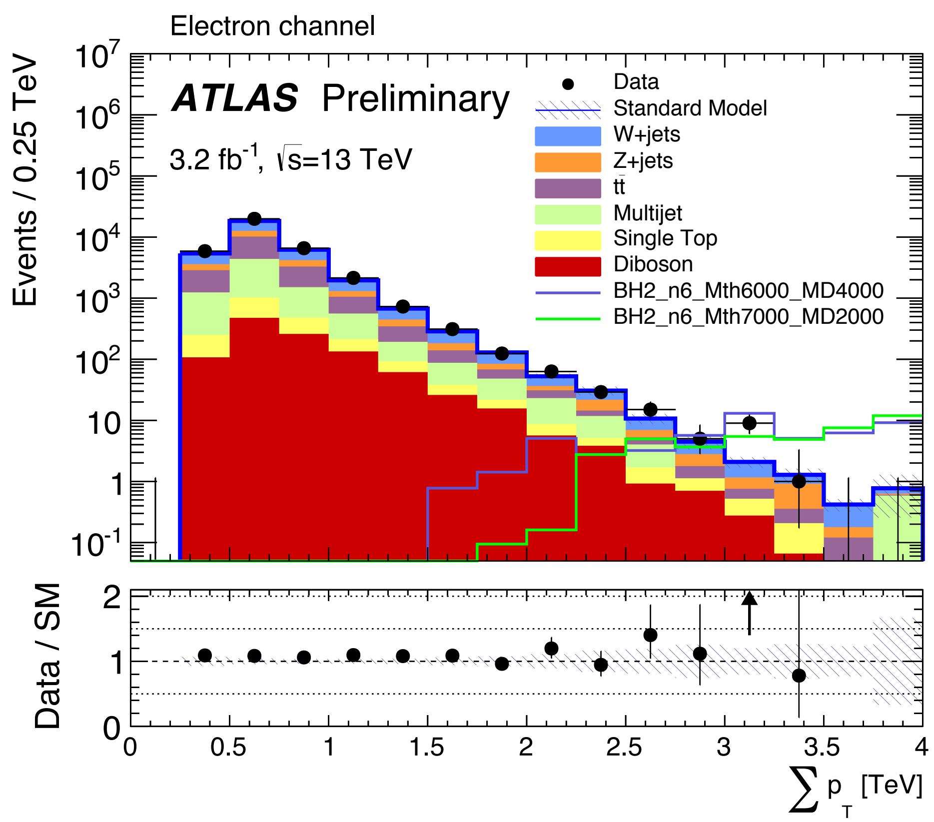

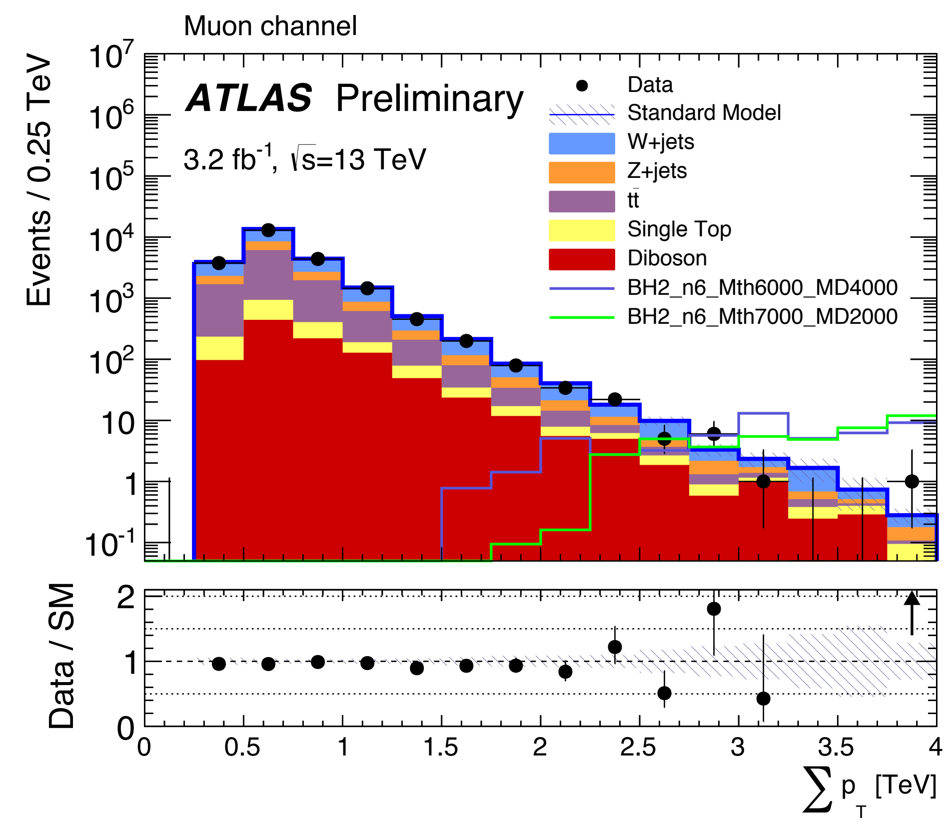

ATLAS search for strong gravity in l+jets

Cut	Control Regions		
	Z+**jets**	W+**jets**	$t\bar{t}$
$\sum p_{\mathrm{T}}$	750–1500 GeV		
Number of Objects	The event must contain at least 3 objects (leptons or jets) with $p_{\mathrm{T}} > 60$ GeV.		
Leading lepton	The event must contain a leading electron or muon of good quality, isolated and with $p_{\mathrm{T}} > 60$ GeV.		
m_{ll}	80 – 100 GeV	n/a	
$E_{\mathrm{T}}^{\mathrm{miss}}$	n/a	> 60 GeV	n/a
Number of leptons	exactly 2, opposite sign same flavour	exactly 1	
Number of b-tagged jets	n/a	exactly 0	> 1
Number of jets	n/a		> 3